NPS ARCHIVE
1966
HYDINGER, R.

THE MEASUREMENT OF OIL FILM THICKNESS VERSUS TIME UNDER IMPACT LOADING CONDITIONS

ROBERT MARLIN HYDINGER

LIBRARY
NAVAL POSTGRADUATE SCHOOL
MONTEREY, CALIF. 93940

S-212

THE MEASUREMENT OF OIL FILM THICKNESS VERSUS TIME UNDER IMPACT LOADING CONDITIONS

by

Robert Marlin Hydinger
Lieutenant, United States Navy
B. S., United States Naval Academy, 1959

Submitted in partial fulfillment
for the degree of

MASTER OF SCIENCE IN MECHANICAL ENGINEERING

from the

UNITED STATES NAVAL POSTGRADUATE SCHOOL
May 1966

NPS ARCHIVE
1966
HYDINGER, R.

Thesis
H975
c.1

ABSTRACT

The thickness of lubricant films under impact loading conditions has been measured as a function of time by passing a collimated beam of light through the film, detecting the emerging rays with a photo-multiplier tube, and displaying the transient waveform on a cathode ray oscilloscope. It is shown that rotative speed is the dominant variable in the determination of film thickness in the contact area of rolling cylinders. Plateau Time is defined as the time period during which minimum film thickness is maintained at the contact area and is interpreted as a measure of the "oiliness" of a lubricant.

Library
U.S. Naval Postgraduate School

TABLE OF CONTENTS

Section		Page
1.	Introduction	7
2.	Test Unit Design Considerations	9
3.	Test Unit Configuration	11
4.	Test Unit Calibration	33
5.	Selection of Lubricants	36
6.	Experimental Procedure	37
7.	Experimental Observations	39
8.	Discussion of Results	51
9.	Conclusions	60
10.	Acknowledgements	61
11.	Bibliography	62
Appendix I - Lubricant Specifications		66
Appendix II - Frictional Drag Estimates		68
Appendix III - Correlation of Pendulum Drop Position and Load		73
Appendix IV - Application of Test Results to Determination of Change in Viscosity		76

LIST OF ILLUSTRATIONS

Figure		Page
1.	Testing Device	12
2.	Rotating Test Surface	13
3.	Clearance Adjusting Plate	14
4.	Tachometer Connection	15
5.	Impact Loading Device	16
6.	Pendulum Positioning Device	18
7.	Lateral Adjusting Nuts	19
8.	Light Source and Optical System	21
9.	Spectral Sensitivity Characteristic of Type 5819 Multiplier Phototube	22
10.	Schematic Arrangement of Type 5819 Multiplier Phototube	24
11.	Anode Characteristics of Type 5819 Multiplier Phototube	25
12.	Sensitivity and Amplification Characteristics of Type 5819 Multiplier Phototube	26
13.	Effect of Magnetic Field on Anode Current	29
14.	Block Diagram of Instrumentation Interconnections	31
15.	Instrumentation	32
16.	Micrometer Positioning Device	34
17.	Calibration Curves	35
18.	Film Thickness vs Rotative Speed for 2110TH Oil	52
19.	Film Thickness vs Rotative Speed for 2190TEP Oil	53
20.	Film Thickness vs Rotative Speed for Versilube F-50	54
21.	Plateau Time vs Rotative Speed, Drop Position 7°	56

Figure		Page
22.	Plateau Time vs Rotative Speed, Drop Position 11.75°	57
A1.	Viscosity vs Temperature for Test Lubricants	67
B1.	Frictional Torque vs Radial Load	72

1. Introduction.

The thickness of the oil film separating the load carrying surfaces in many machine elements, in relation to the roughness of the surface, determines the state of lubrication. The efficient operation of these machine elements is critically dependent upon the state of lubrication. If the lubricant film becomes too thin, direct metallic contact may take place leading to wear or seizure of the surfaces.

Many theories have been postulated to predict the minimum film thickness under varying load conditions. Such a theory is essential for a rational design of machine elements such as gears and rolling bearings. However, a complete and adequate theory of elasto-hydrodynamic lubrication is not yet available. Grubin [15] has presented one of the most general theories while Dowson and Higginson [19] have advanced perhaps the most developed and most accurate of the recently published theories. It must be noted, however, that a theory is only good to the extent that it may be substantiated by experimental evidence.

The accurate measurement of film thickness under operating conditions is, by its very nature, not easy to accomplish. Numerous methods have been used in the past with varying degrees of success. Christensen [6] determined film thickness by measuring directly the displacement relative to the machine frame of a lightly loaded pad riding on the surface film ahead of the contact. El Sisi and Shawki [20] used an additive in the lubricant to increase its electrical conductivity and an electrical resistance method of measurement. Cameron and MacConochie [22] maintained a continuous electric discharge between gear tooth surfaces at the point of minimum oil film thickness. The voltage required to maintain

the discharge was proportional to the film thickness. Borsoff and Wagner [10] dissolved radioactive sulfur in the libricant which formed an E.P. film on the gears tested. The radioactivity on the working surfaces was measured using a thin window G-M tube and by autoradiography methods and was related to film thickness. Klorig [41] used a light measurement technique similar in principle to the x-ray technique used by Sibley and Orcutt [14].

Of the methods mentioned above, those based on electrical resistance and conductivity have been subject to considerable skepticism due to the fact that precise rheological data on lubricants under high pressure is not available. The method used by Klorig showed promise of successful and relatively direct application if a system of sufficient sensitivity could be developed for detecting the light signal. The only apparent drawback in this method is the change in optical absorption of the lubricant under pressure. While no data are available for typical lubricants, Bridgman [36] has stated that tests on various aqueous salt solutions yielded no striking effects on absorption under high pressures. Collins [37] made similar tests on water, methyl alcohol, and toluene with the results that no changes were found either in the spectral position or the intensity of the absorption bands studied. With this information, it appears reasonably safe to proceed on the assumption that increased pressure will have little or no measurable effect on optical absorption.

The object of this investigation is to utilize the light measurement technique for determination of oil film thickness as a function of time under conditions of impact loading, and to correlate the results with existing elasto-hydrodynamic theory.

2. Test Unit Design Considerations

The basic requirement for conducting the proposed research was a testing device for measuring thin oil films. Preliminary considerations indicated that the device should consist of:

(a) A rotating test surface with rigid mounts capable of withstanding high impact loads while sustaining minimum deformation.

(b) A means of impact loading to squeeze the oil film on the test surface to minimum thickness.

(c) A light source of sufficient intensity and directional capabilities to pass through the oil film and be detected.

(d) A detection device for the light signal.

(e) A recording device for the detected signal.

(f) An electronic unit for synchronizing the events of the test.

To avoid the necessity of designing a separate machine in the future for further research in this field, an additional capability was built into the testing apparatus to provide for measurement of the change in viscosity of the lubricant being tested. This latter feature dictated, to a degree, the specifications for the test surface and the loading device.

The estimate of minimum film thickness to be measured was taken as 0.0005 inches. This value then established a relative set of tolerances for various parts of the testing machine. To bridge the gap of statistical variations in material quality and to minimize vibrational problems, the policy of over-design was used whenever practicable. The

most notable departures from this policy were in the selection of certain bearing sizes where frictional drag calculations were the limiting factors.

3. Test Unit Configuration.

The overall configuration of the testing device is shown in Figure 1.

The rotating test surface (Figure 2) was designed as a stepped shaft of circular cross-section. The massive construction of this shaft is intended to help maintain uniform rotative speed under impact loads. The actual test surface is one-half inch wide and six inches in diameter. The shaft is constructed of AISI 8620 steel, case carburized to 1/16 inch depth with a hardness of 50-60 Rockwell C. The surface finish is ground to six microinches center line average. The shaft is rigidly supported at either end in precision ground tapered roller bearings. Provision was made for adjusting the axial and radial clearances in these bearings by means of a clearance adjusting plate, shown in Figure 3. The shaft was coupled, by means of a flexible coupling, to a variable speed d-c drive motor. The flexible coupling was employed, rather than belt drive, to minimize transverse vibrations from the drive source. To measure the shaft rotative speed, a tachometer was geared directly to the shaft adjacent to the flexible coupling (Figure 4).

The impact loading device was configured as a compound pendulum. This is shown in Figure 5. The weight at the end of the pendulum is so designed as to position the point of impact at the center of precussion of the pendulum. This, of course, eliminates any reaction at the pivot point due to impact. The large wheel at the end of the pendulum arm is a free rotating wheel of AISI 8620 steel ground to a six microinch center line average finish. The specifications for this part are identical to those of the test surface on the main shaft with which it comes into

FIGURE 1.
Testing Device

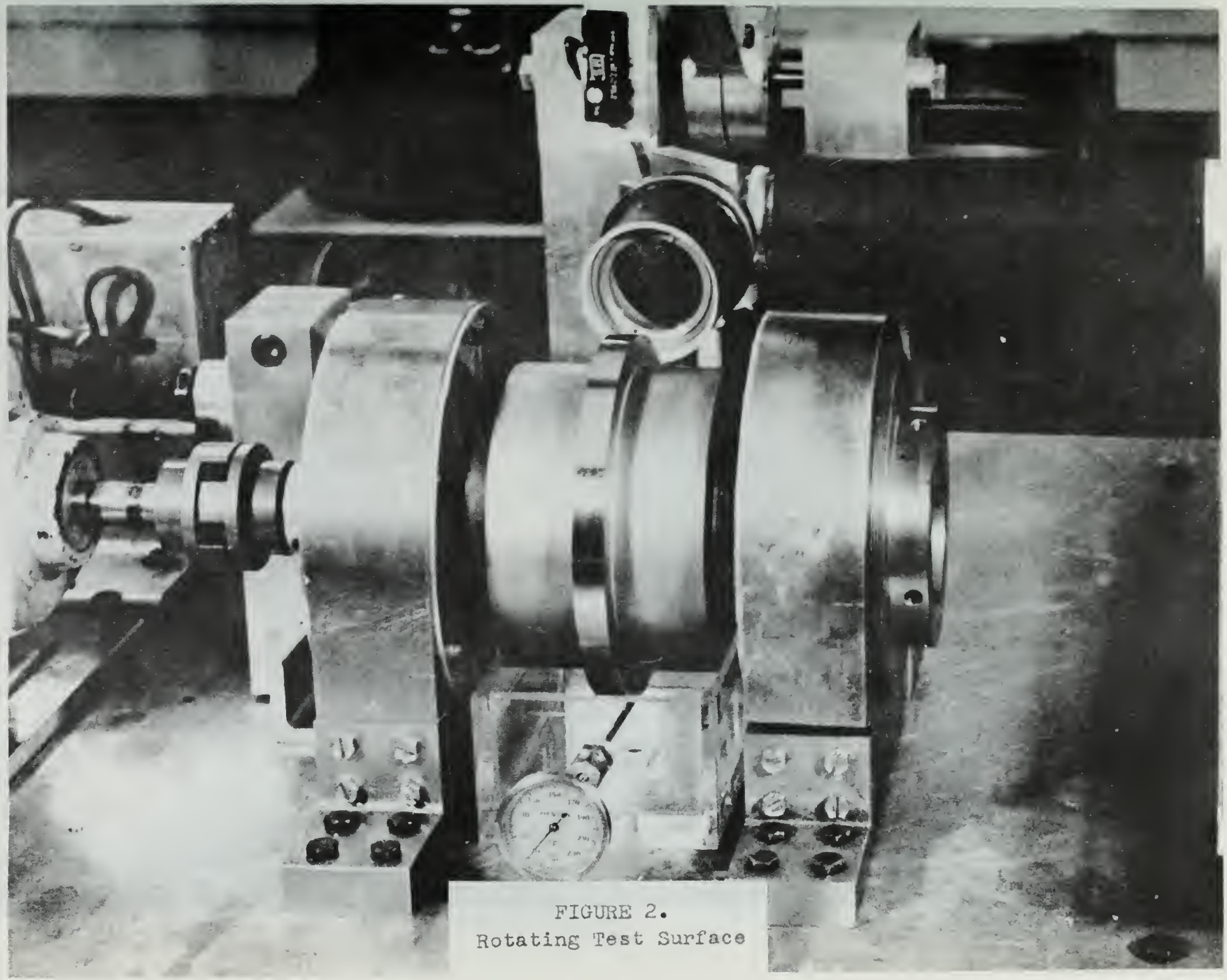

FIGURE 2.
Rotating Test Surface

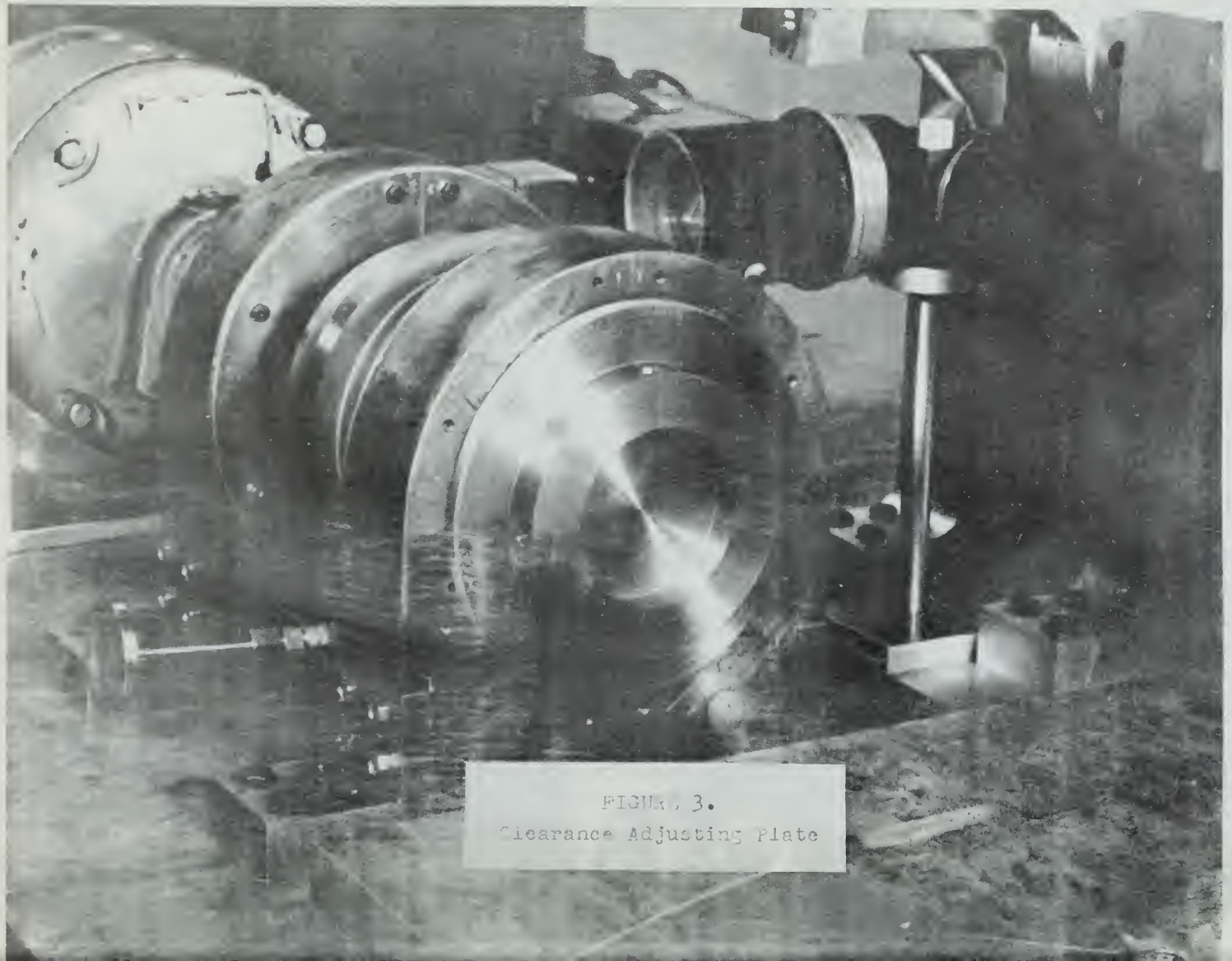

FIGURE 3.
Clearance Adjusting Plate

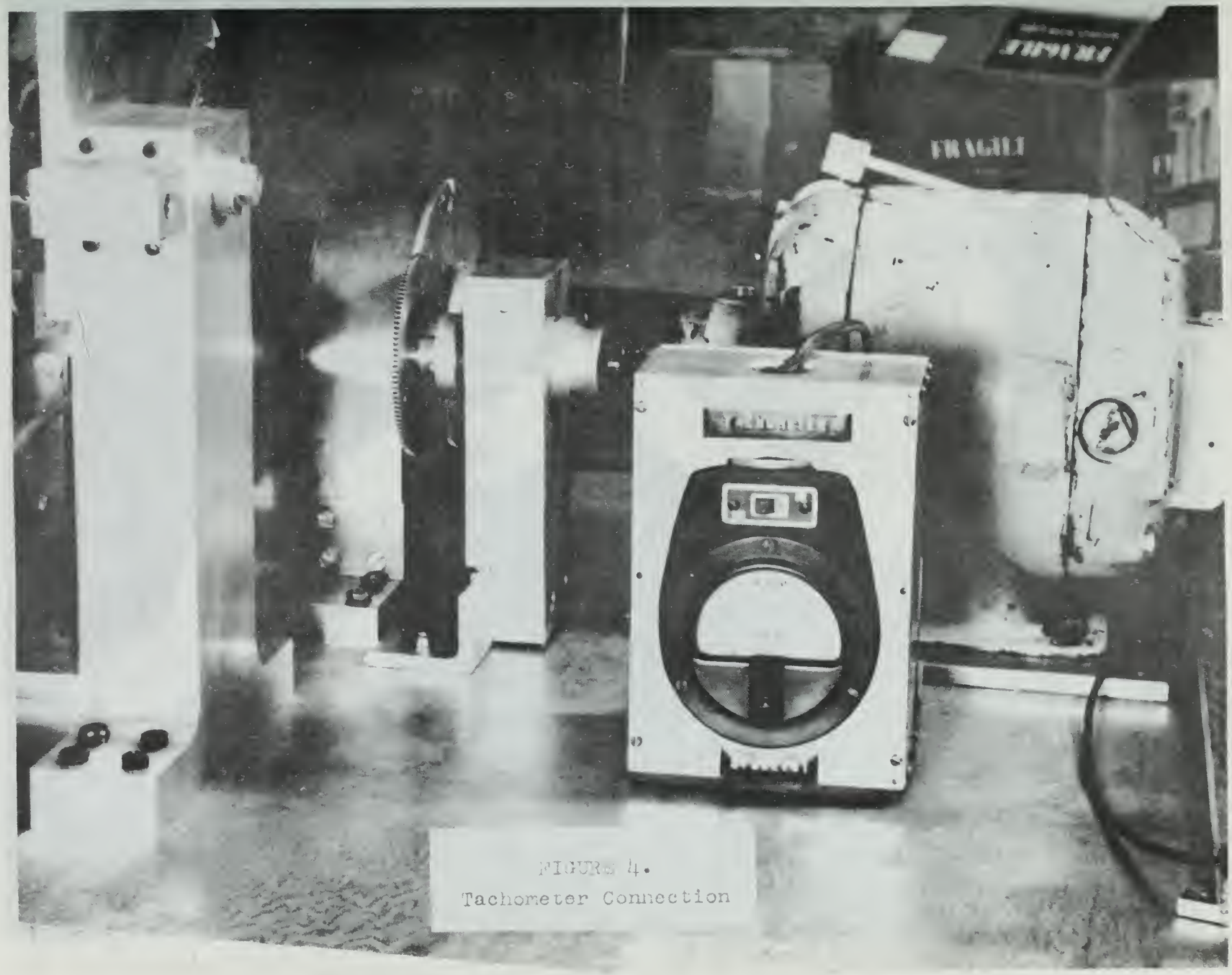

FIGURE 4.
Tachometer Connection

FIGURE 5.
Impact Loading Device

contact during testing.

The bearings supporting this wheel are sized such that their frictional drag will be negligible compared to the viscous drag in the lubricant on the test surface of the wheel subsequent to impact. This consideration was necessary to validate the measurement of change in viscosity of the lubricant. See Appendix II for these calculations.

The overall mass of the pendulum was great enough that a gravity drop was sufficient to provide the desired impact loading. Gravity drop from a specified height has the additional advantage of being reproducible on multiple tests. To position the pendulum, a ratchet was built into the hub around the pivot point. This is shown in Figure 6. The pendulum position is read from a graduated and calibrated scale attached to a supporting member.

Adjustment for parallel alignment of the two rotating test surfaces was accomplished by using a ball and socket mounting at the pivot point of the pendulum which allows rotation about the longitudinal axis. Lateral alignment is affected with two adjusting nuts in the pendulum supports (Figure 7).

The selection of a light source was based on two primary requirements:

(1) Sufficient intensity
(2) Stable output

The intensity requirement was directly related to the sensitivity of the signal detection equipment. Hence, those two design parameters were considered jointly. The detection device was so chosen as to place no stringent requirement on the intensity of the source. This eliminated a rather formidable problem area, inasmuch as the vast majority of high

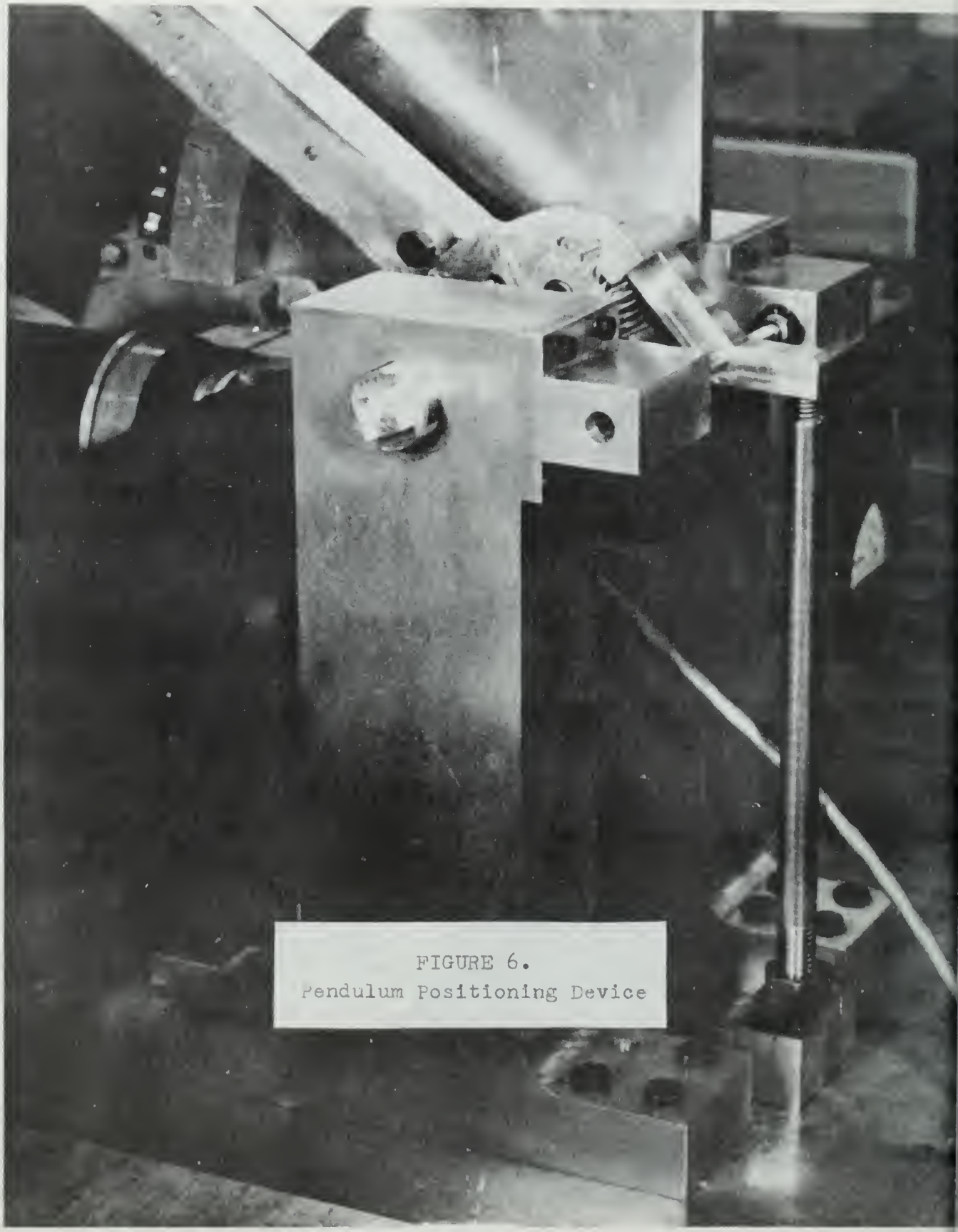

FIGURE 6.
Pendulum Positioning Device

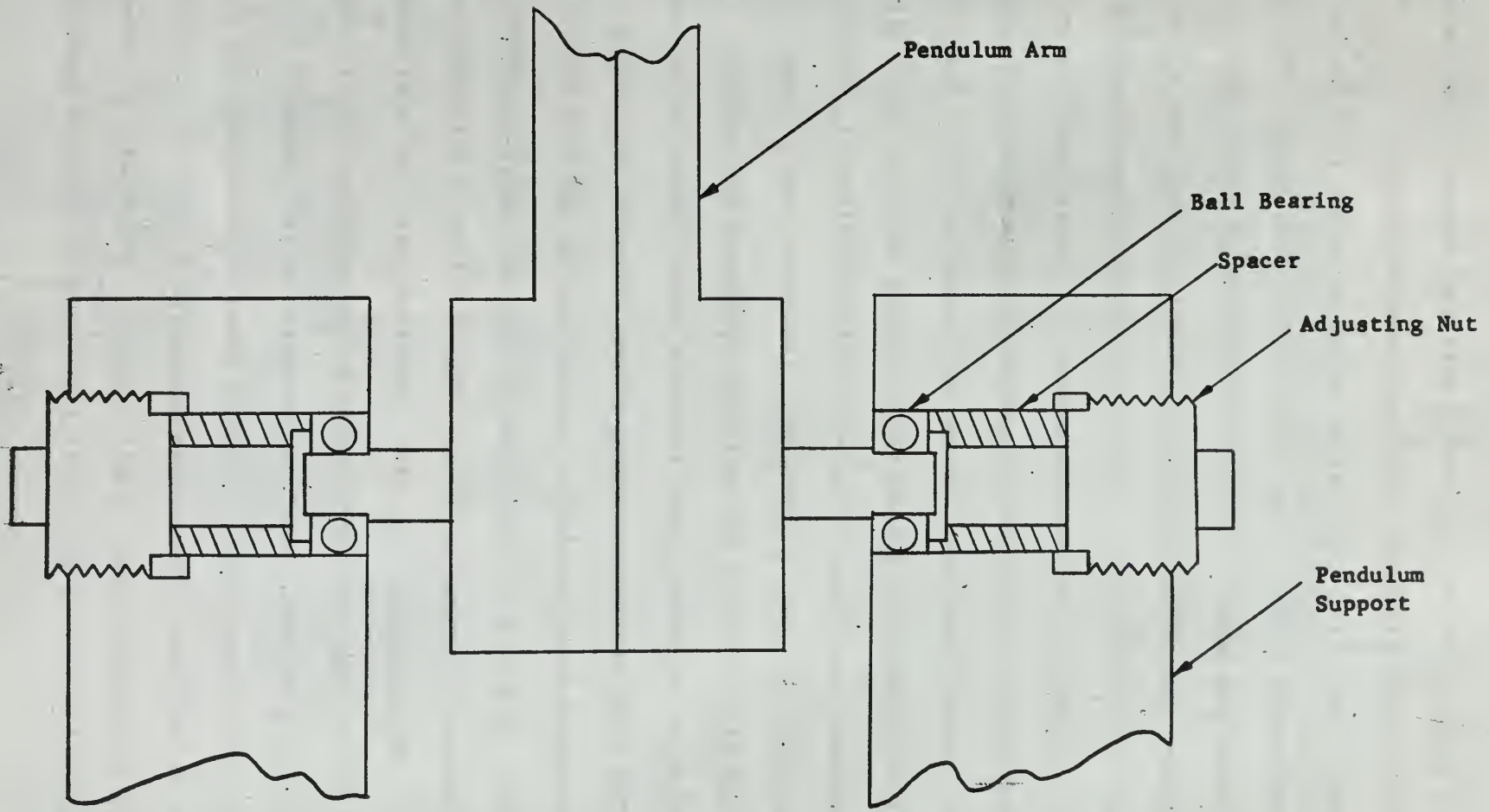

FIGURE 7.

ADJUSTING NUTS FOR LATERAL ALIGNMENT

intensity sources have an unsteady or pulsating output. This includes the variety of arc discharge lamps and tubes available.

Output stability (no flicker or cyclic variation in light intensity) was a requirement levied by the duration of a "test event". The time involved in any one measurement of film thickness is of the order of several milliseconds. Any variation in light intensity during such a period would invalidate the measurement. A perfectly steady d-c source would provide the only assurance of reliable operation. Full wave rectification and filtering of an a-c signal was determined to be unsatisfactory within feasible limits. Therefore, two wet cell batteries of 175 ampere-hour capacity were connected in parallel to provide power for the light source. A further assurance of steady output would be realized if a heavy tungsten filament could be used. A microscope illuminator with a ribbon filament, type SR-8, rated at six volts and 18 amperes was selected. This was coupled to an optical train for point source generation and collimation. The light source and optical system are shown in Figure 8.

The signal detection device selected was the RCA 5819 Multiplier Phototube. This is a 10-Stage, head-on type of high vacuum phototube with an S-4 spectral response as shown in Figure 9. Maximum response occurs at 4000 $\pm$ 500 angstroms. The 5819, therefore, has high sensitivity to blue light and negligible sensitivity to red radiation. It is capable of multiplying extremely small photoelectric current produced at the cathode by an average value of 500,000 times when operated with a supply voltage of 1000 volts. The output current is a linear function of the exciting illumination under normal operating conditions. The frequency response of the tube is flat up to a frequency of about 50 megacycles per

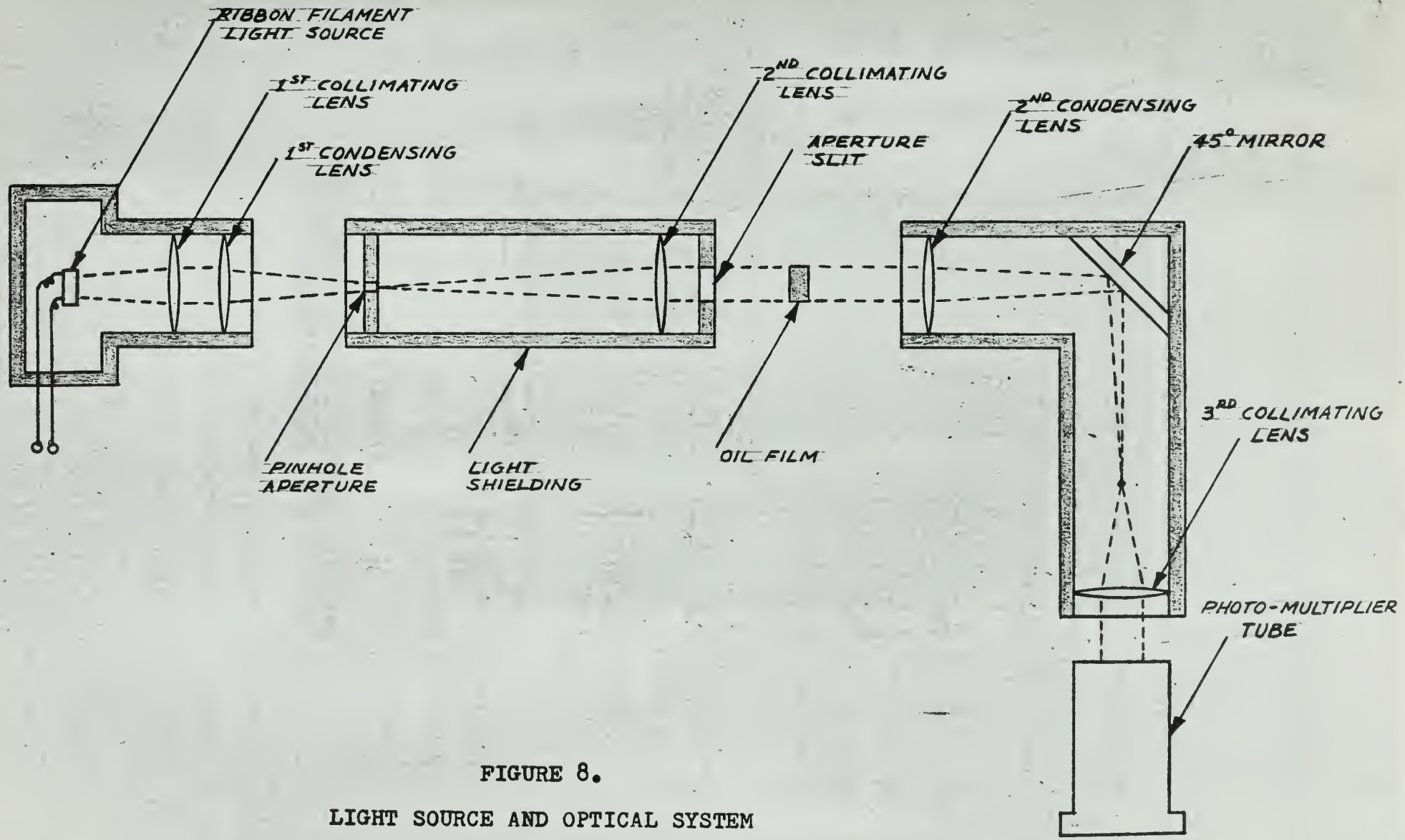

FIGURE 8.

LIGHT SOURCE AND OPTICAL SYSTEM

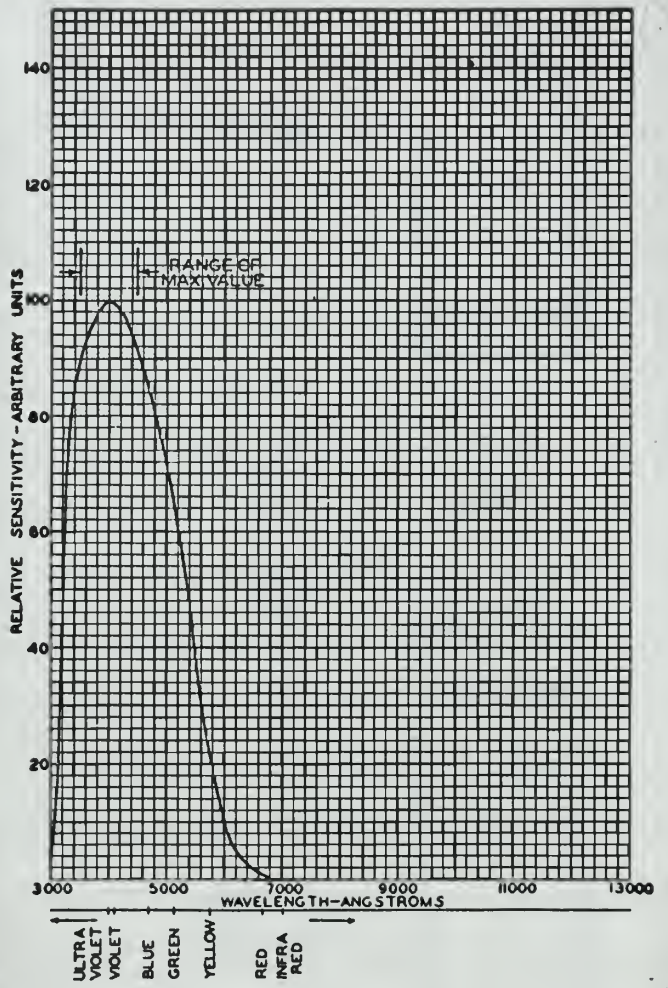

FIGURE 9.

SPECTRAL SENSITIVITY CHARACTERISTIC
OF TYPE 5819 MULTIPLIER PHOTOTUBE

second, above which the variation in electron transit time becomes the limiting factor.

Basically, the multiplier phototube is a vacuum tube which utilizes the phenomenon of secondary emission to amplify signals composed of electron streams. A schematic arrangement of the 5819 is shown in Figure 10. The electrons emitted from the illuminated, semi-transparent cathode are directed by fixed electrostatic fields to the first dynode. These electrons impinging on the dynode surface produce many more electrons, depending on the energy of the impinging electrons. These secondary electrons are then directed by fixed electrostatic fields to the next dynode and the process repeats itself through to the last dynode. The anode collects the electrons emitted from the last dynode and they constitute the current utilized in the output circuit.

The operating stability of the 5819 is dependent upon the magnitude of the anode current and its duration. In general, high values of anode current will induce a fatigue, characterized by a decrease in sensitivity. This decrease is, of course, dependent upon the severity of the operating conditions. After the tube has been stored in darkness for a day or so, the sensitivity will usually recover to approximately the initial level. From this discussion, it is obvious that the average anode current used must be held to a value well below the maximum rated value for the tube to ensure stability. The average anode characteristics for the tube are shown in Figure 11.

The range of sensitivity of the tube is dependent upon the respective amplification of each dynode stage which is in turn dependent on the supply voltage per stage. The sensitivity and amplification characteris tics of the tube are shown in Figure 12.

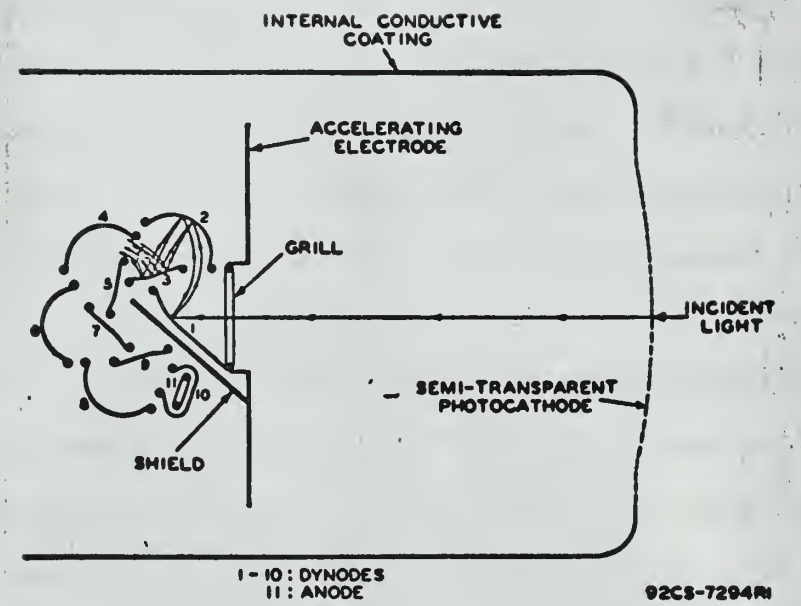

FIGURE 10.

SCHEMATIC ARRANGEMENT OF TYPE 5819 MULTIPLIER PHOTOTUBE

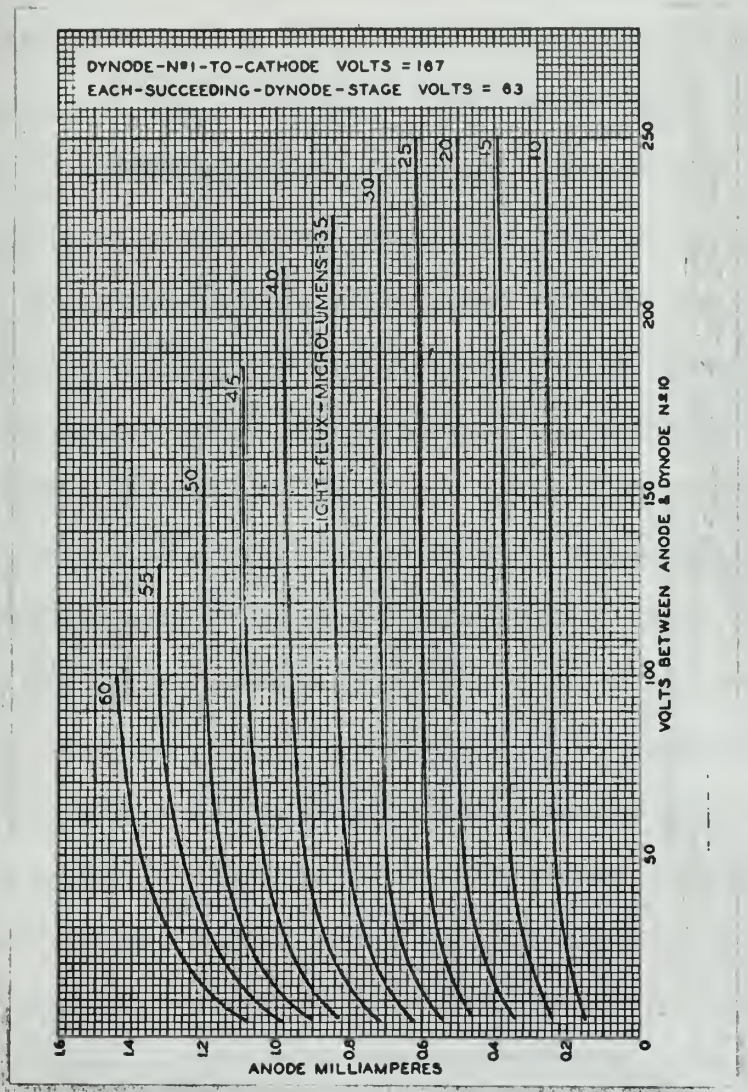

FIGURE 11.

ANODE CHARACTERISTICS OF TYPE
5819 MULTIPLIER PHOTOTUBE

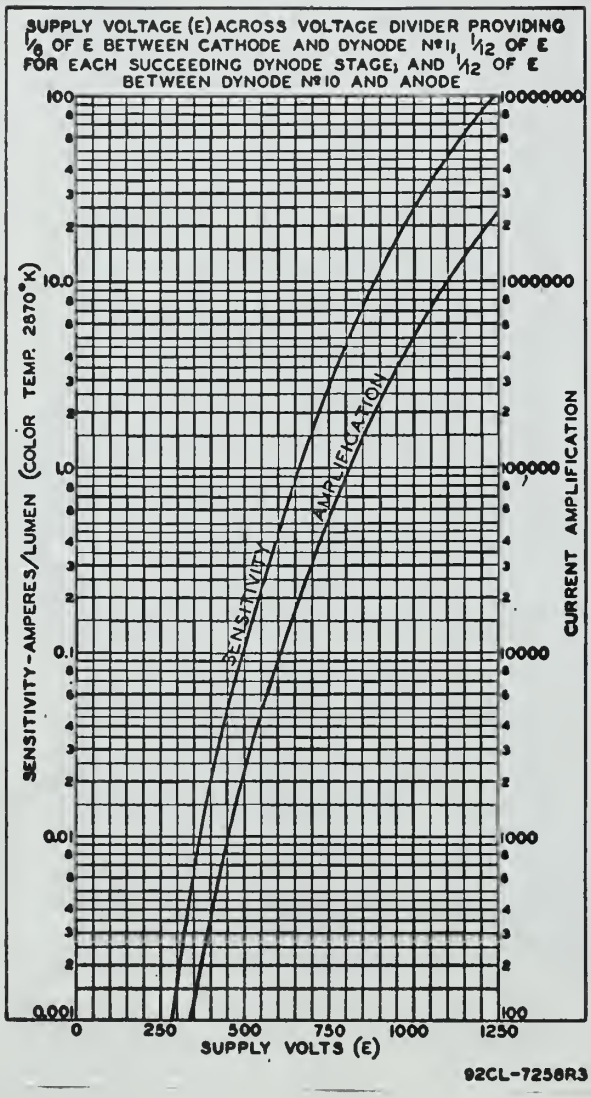

FIGURE 12.

SENSITIVITY AND AMPLIFICATION CHARACTERISTICS OF TYPE 5819 MULTIPLIER PHOTOTUBE

In utilizing the tube, one strives primarily for stability of operation and a high signal to noise ratio. Stability, as previously noted, is a function of anode current. High signal to noise ratio implies a high sensitivity and low dark current. These two factors are, however, contradictory to a certain degree. From Figure 12, it is apparent that sensitivity increases with supply voltage. On the other hand, dark current increases with voltage per stage. At this point, it would be well to discuss the phenomenon of dark current. There are three domains in each of which a different type of dark current dominates. These dark currents are caused by (a) ohmic leakage, (b) amplified thermionic emission, and (c) regenerative ionization. Ohmic leakage dominates up to about 50-60 volts per stage. Above 60 volts per stage, thermionic emission becomes important. In almost any method of using the multiplier phototube, the ultimate limiation to signal detection is thermionic emission. Associated with this component of the dark current is a shot noise resulting from random thermionically emitted electrons, variably multiplied by the secondary emission gains of all stages. Above about 110 volts per stage, a third region of dark current begins which is associated with regenerative ionization effects and which causes complete breakdown and an uncontrollable discharge at sufficiently high voltage. Hence, the desirable combination of high sensitivity and low dark current is, at best, a problem of optimization. Selection of the 5819 takes a considerable amount of the sting out of the problem, since this particular tube has an uncommonly high signal to noise ratio when operated in a normal range below 1000 volts.

Considering the spectral characteristic of the light source used, it may give the reader some concern that a phototube with a spectral

sensitivity centered further up the wavelength scale was not selected. The chief justification for this lies in the fact that the 5819 is so much more sensitive than its competitor in the 5500 angstrom range. In fact, they differ by a factor as high as 25.

With certain orientations of the 5819, the earth's magnetic field is sufficient to cause a noticeable decrease in the response of the tube. Figure 13 shows the effect on the anode current of variation in magnetic field strength. To prevent this decrease in response, the tube was fitted with a combination magnetic and electrostatic shield. Electrostatic shielding was necessary to prevent internal discharge phenomena at high voltages which would result in an increase in noise.

The selection of a recording device for the signal from the photomultiplier tube was limited by system response requirements. As previously mentioned, the entire test event would encompass only a few milliseconds. Practically speaking, this eliminated an electro-mechanical device from the possible choices. An oscilloscope with a memory circuit, however, would satisfy response requirements and would permit photographic reproduction of the test results. A Memo-Scope oscilloscope was used for this purpose. Traces were then photographed at leisure using a panchromatic film rated at ASA 200. This provided well defined copies of each test result.

Synchronization of the triggering pulse for the oscilloscope was provided by a pulse generator operating in conjunction with a microswitch tripped by the pendulum arm. The delay between closing the microswitch and triggering the oscilloscope was adjusted by varying the output pulse width of the pulse generator. The generator output was a

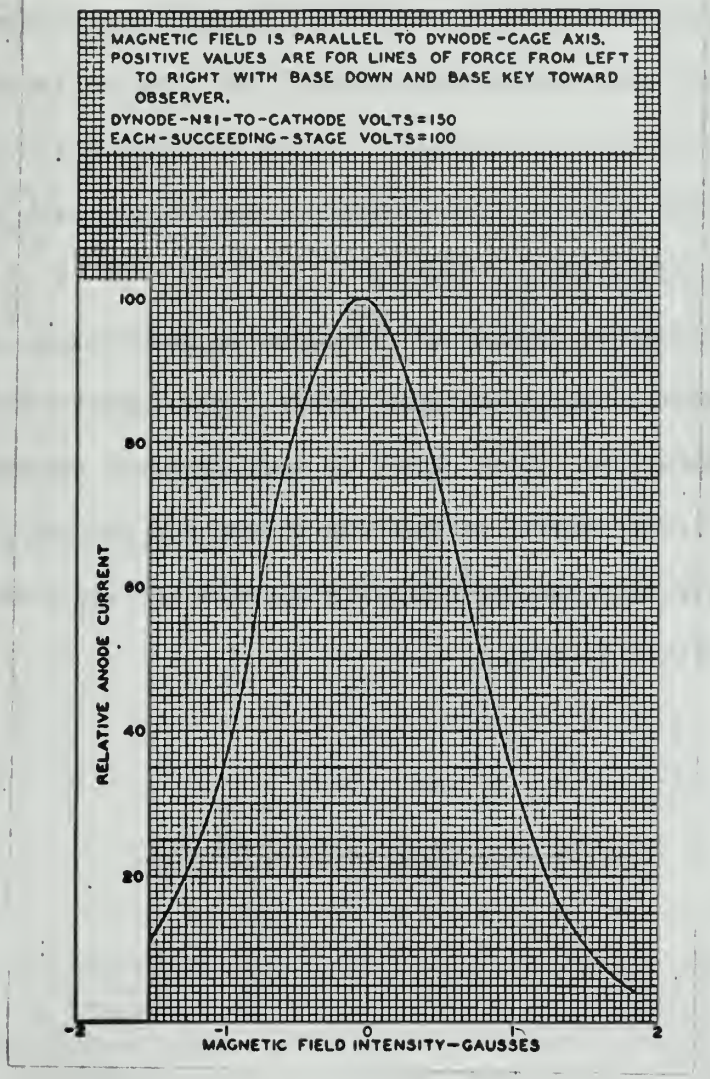

FIGURE 13.

EFFECT OF MAGNETIC FIELD
ON ANODE CURRENT

positive square wave form that tripped to a negative value at termination. A block diagram of the instrumentation interconnections is shown in Figure 14. Thus, the scope could be set to trigger on a negative signal after a predetermined delay which could be varied from 0.1 microsecond to 1.0 second. With such precise synchronization, the time scale on the oscilloscope could be adjusted to present a trace of optimum size. Figure 15 shows the oscilloscope and pulse generator, in company with the power supply for the photomultiplier tube.

Vibrations from the impact of the pendulum head posed a potential problem. To minimize this, the table holding the impact device was mounted on a composition rubber sheet of approximately one-half inch thickness. The light source, channeling system and photomultiplier tube were placed on separate tables similarly mounted and all electronic equipment was individually located.

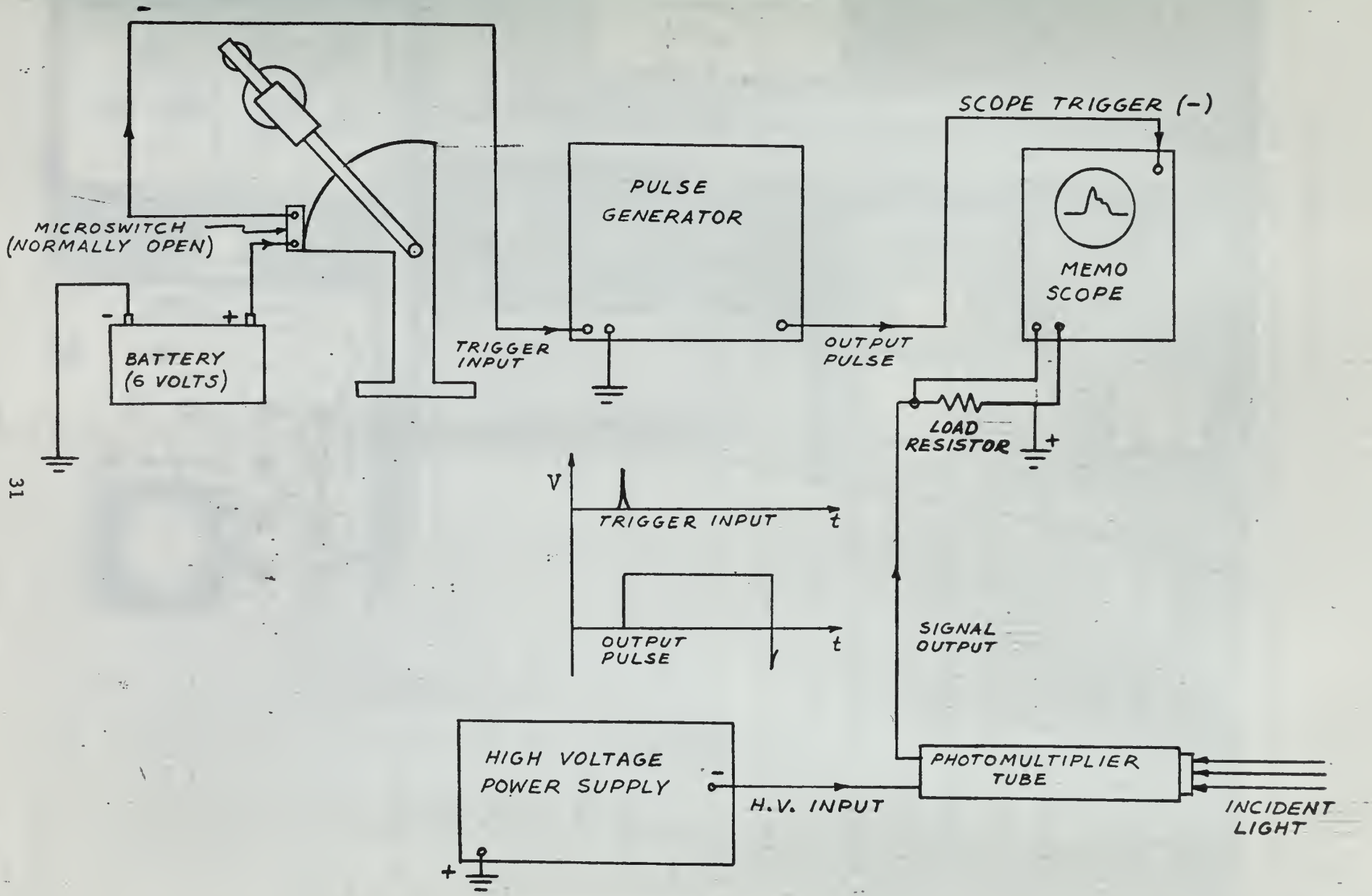

FIGURE 14

BLOCK DIAGRAM OF INSTRUMENTATION INTERCONNECTIONS

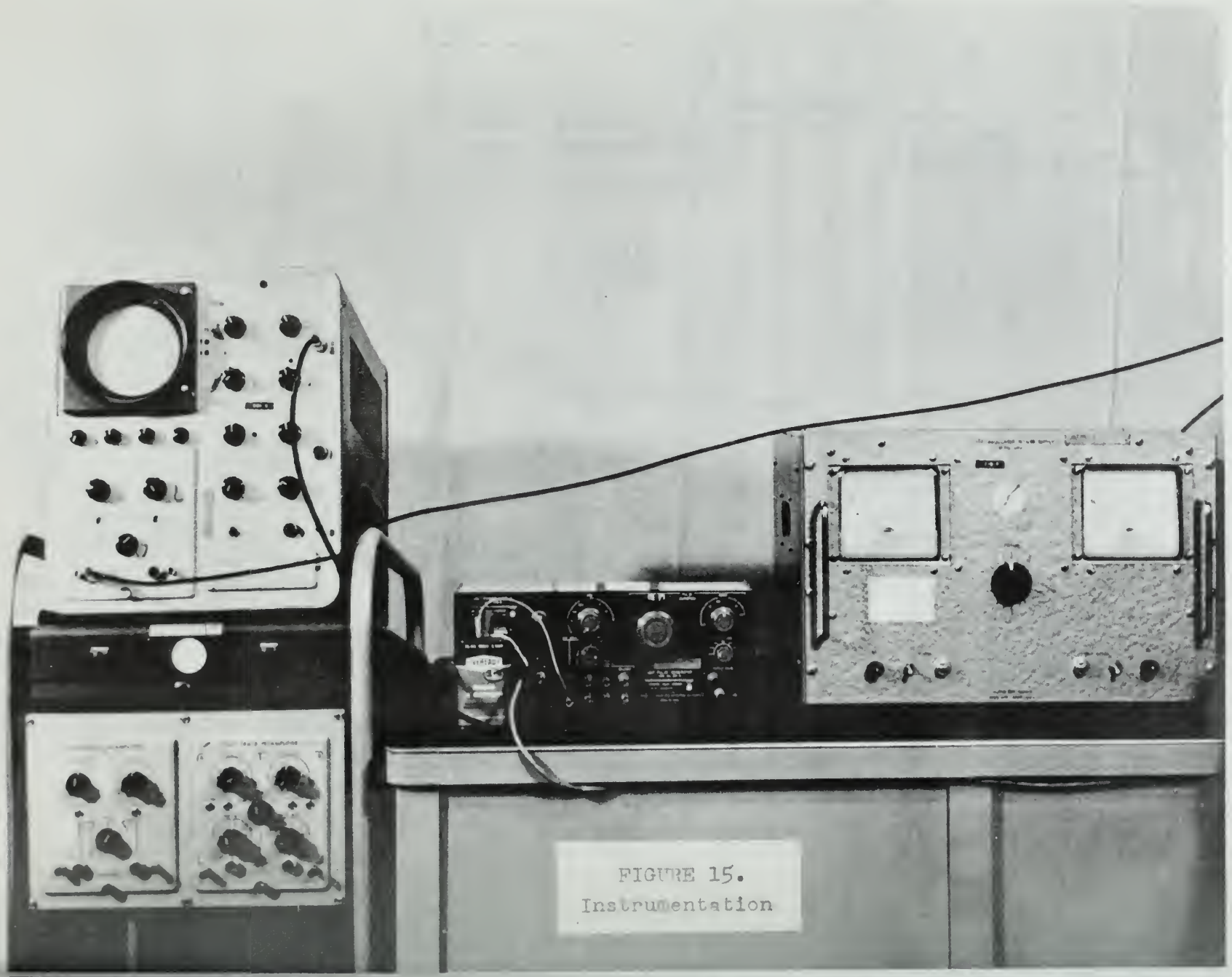

FIGURE 15.
Instrumentation

4. Test Unit Calibrations.

The purpose of test unit calibration was to establish a relation between the output of the photomultiplier tube and light passing through the lubricant film. The output of the tube is directly proportional to the amount of light incident on the cathode. Light passing through the lubricant film is directly proportional to the thickness of the film (since the face width of the test surface is constant). Therefore, with the tube operating in a linear region, the output should be directly proportional to the film thickness. The calibration then should consist of setting a known value of disc separation, with the lubricant film present, and measuring the tube output across the load resistor. The disc separation was set with an adjustable micrometer positioning device shown schematically in Figure 16. The gap between the discs was then measured using a microscope. This microscope, with an etched hairline on one reticle, could be adjusted in the vertical plane with a calibrated vernier, enabling one to measure the separation between the two surfaces of the discs. The vernier could be read to an accuracy of 0.001 mm. Thus, the micrometer was calibrated to read gap thickness corresponding to a given setting. Lubricant was placed on the test surfaces, the light source was energized, and the output signal was read from the oscilloscope for preset gap thicknesses. A calibration curve was obtained for each lubricant tested so as to account for any variation in light attenuation properties among the lubricants. These calibration curves are shown in Figure 17.

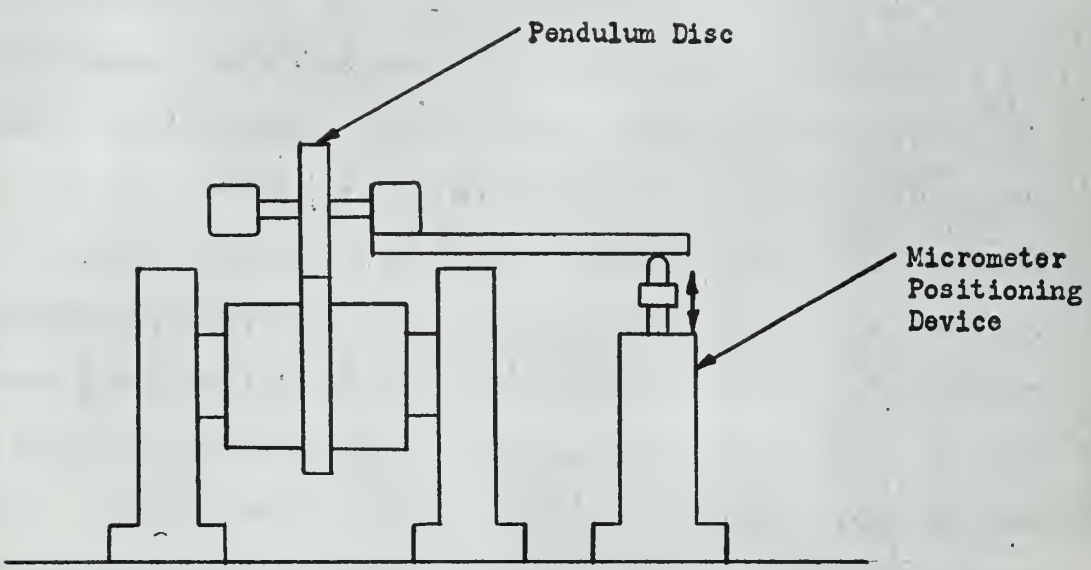

End View

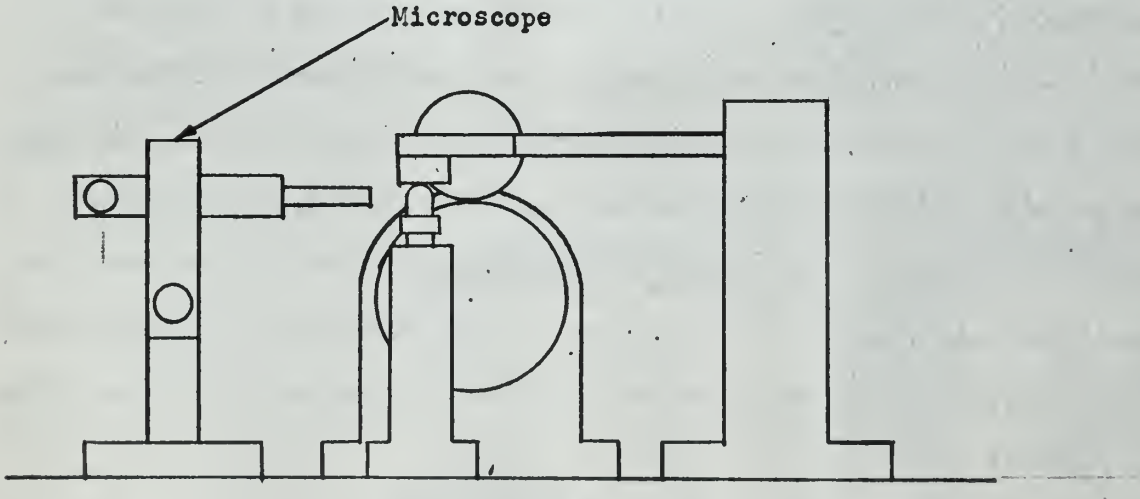

Side View

FIGURE 16.

MICROMETER POSITIONING DEVICE

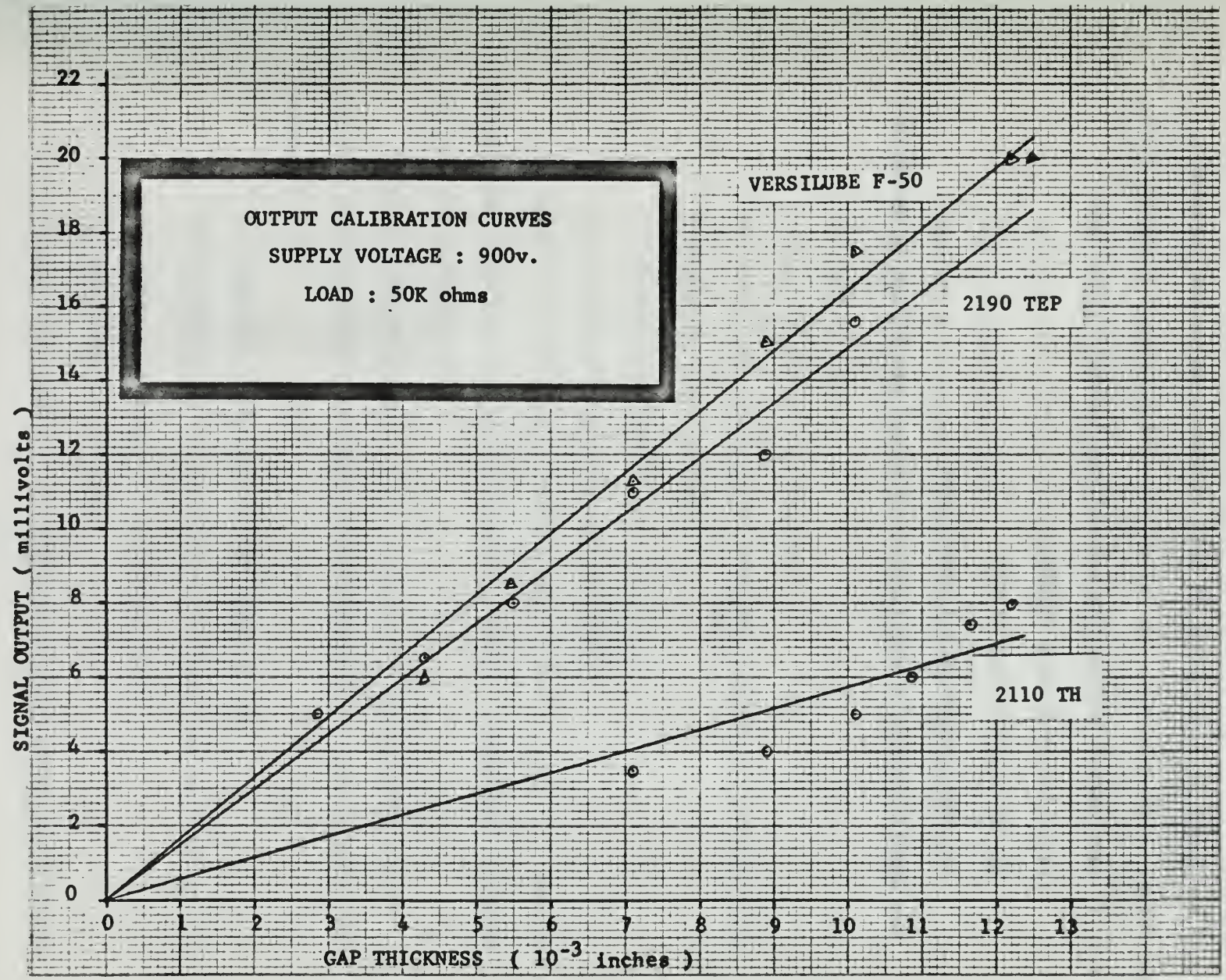

FIGURE 17.

CALIBRATION CURVES

5. Selection of Lubricants.

The criteria established for the selection of lubricants to be tested was based on a variation of bulk viscosity and other physical properties. With this aim, the following lubricants were obtained from the U. S. Navy Marine Engineering Laboratory, Annapolis, Maryland:

(a) Military Symbol 2190TEP

(b) Military Symbol 2110TH

(c) Versilube F-50 Silicone Fluid

The specifications of the lubricants tested are listed in Appendix I.

6. Experimental Procedure.

The basic instrumentation previously described, and shown schematically in Figure 14, was employed and the experimental procedure reduced to the following sequence:

(a) Clean test surfaces with acetone.

(b) Apply lubricant to surfaces.

(c) Set pendulum height.

(d) Set pulse width for synchronized delay period.

(e) Set drive motor speed at constant preselected value.

(f) Darken room.

(g) Arm sweep on oscilloscope.

(h) Bring photomultiplier tube power supply up to 900 volts.

(i) Turn on light source.

(j) Release pendulum.

(k) Photograph trace on oscilloscope.

It should be noted that a calibration of pulse width as a function of pendulum drop position was performed in order to maximize the trace size on the oscilloscope.

Special precautions were taken to minimize the introduction of spurious light signals into the photomultiplier tube. These consisted primarily of:

(a) Complete shielding of the light source.

(b) Shielding of the photomultiplier tube and optical train.

(c) Light shielding of the testing room.

(d) Operation after dark.

To eliminate the effect of reflections passing around the edge of

the test surfaces when "zero" gap thickness was set, the d-c level of the oscilloscope was reset to zero. The aforementioned preparations yielded an output signal free from all extraneous signals except circuit noise. This noise was of such a nature that it could not be completely eliminated, but only minimized within practicable limits.

7. Experimental Observations.

Observations of experimental results will be presented in photographic form showing the variation of film thickness with time. As indicated in Section 5, three lubricants were tested. The conditions of testing, for each lubricant, were as follows:

(a) For a pendulum release height of seven degrees, speed was varied over a range of approximately 200 to 1000 rpm.

(b) For a pendulum release height of 11.75 degrees, speed was varied over the above stated range.

All photographs may be interpreted by recognition of the following facts:

(a) The time scale, running from left to right, is an arbitrary period of time so chosen as to maximize the trace size on the oscilloscope face. Hence, the zero time reference of any photograph does not, and need not, necessarily coincide with that of any other photograph.

(b) The output signal of the photomultiplier tube is negative. Therefore, as the film thickness decreases, the trace will approach the zero magnitude reference line from below it.

(c) The majority of traces start at a value which is beyond the scale set on the oscilloscope. This is clearly an attempt to provide maximum definition at small film thicknesses.

(d) All magnitude scales are presented in millivolts to avoid odd scaling factors. These may be related, to film thickness for each lubricant, using Figure 17. This correlation is presented in Section 8. In addition, each photograph

is annotated with the conversion factor from millivolts to inches of film thickness.

To avoid needless repetition, only a limited number of representative photographic test results will be presented. Series # 1 through # 6 show the effects of varying speed at a constant load for two different loads. Series # 7 shows the dominant effect of high speed. Series # 8 shows elastic rebounds.

Series # 1

Lubricant: 2110TH
Drop Position: 7 degrees

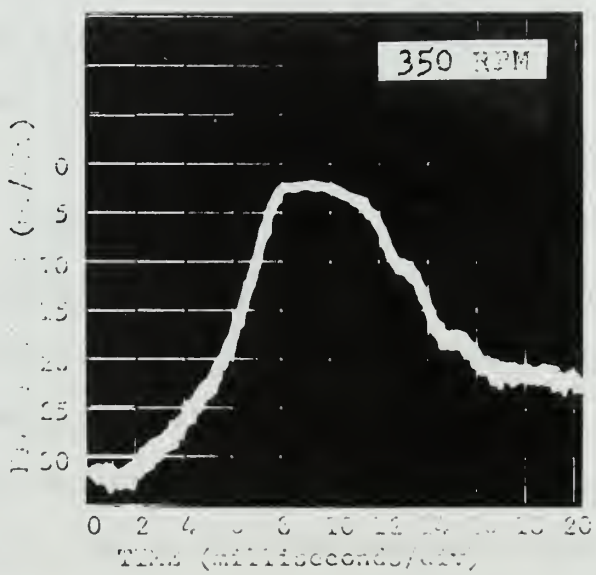

Vertical Scale: 5 mv = 0.0087 inch

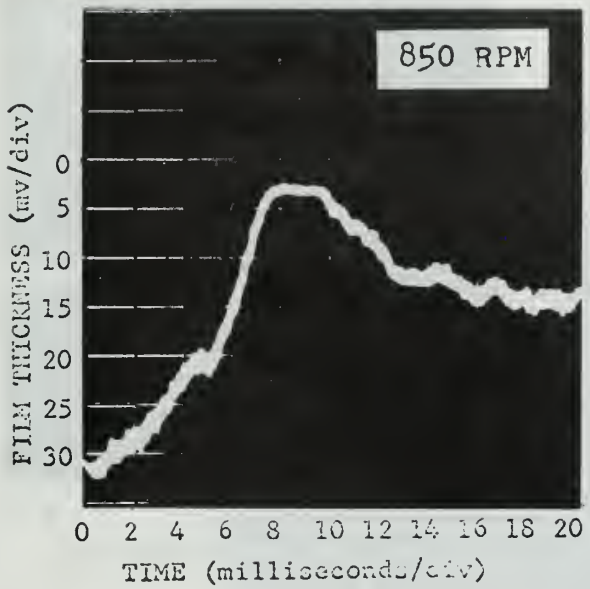

Vertical Scale: 5 mv = 0.0087 inch

Series # 2

Lubricant: 2110TH
Drop Position: 11.75 degrees

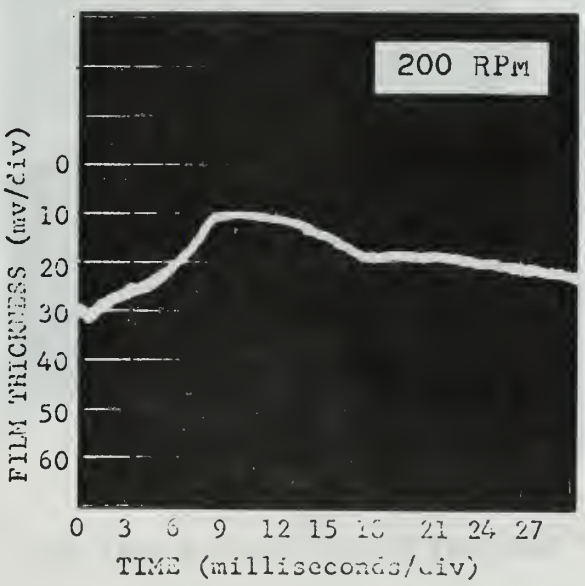

Vertical Scale: 5 mv = 0.0087 inch

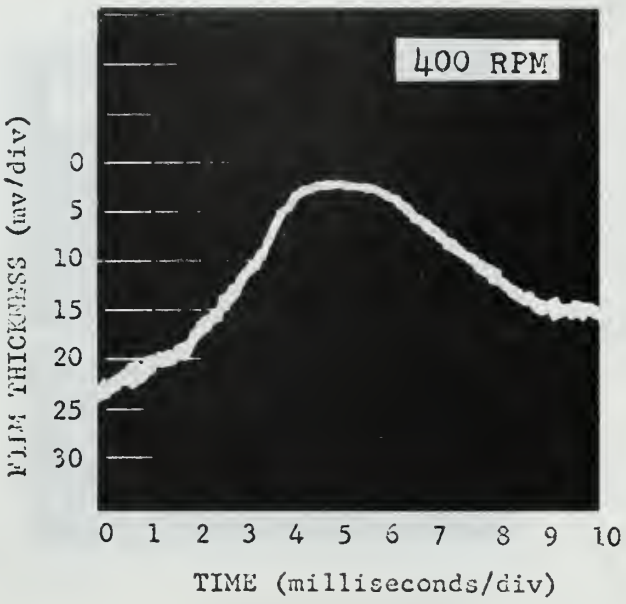

Vertical Scale: 5 mv = 0.0087 inch

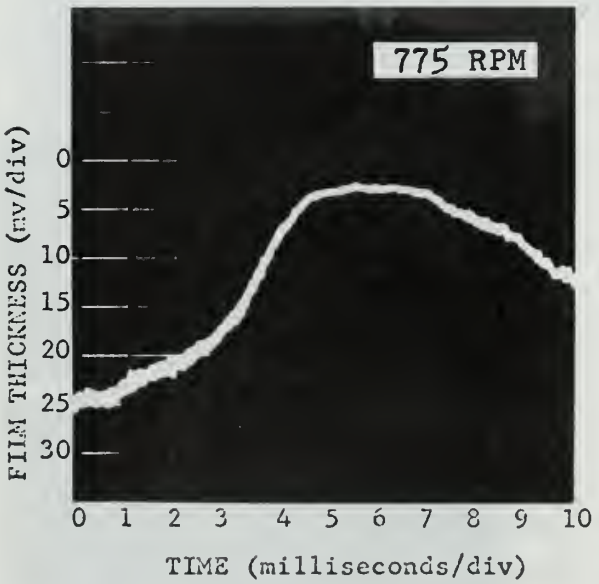

Vertical Scale: 5 mv = 0.0087 inch

Series # 3

Lubricant: 2190TEP
Drop Position: 7 degrees

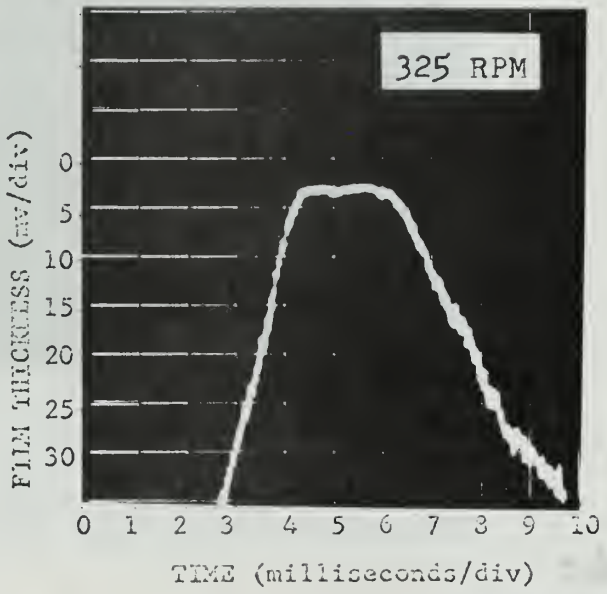

Vertical Scale: 5 mv = 0.0034 inch

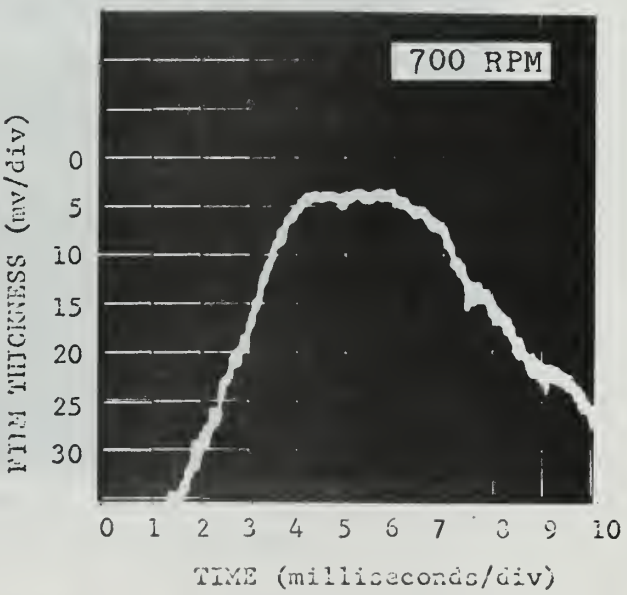

Vertical Scale: 5 mv = 0.0034 inch

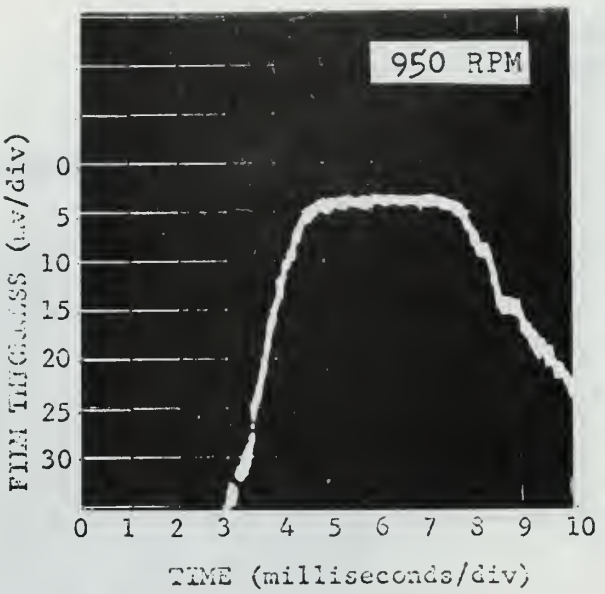

Vertical Scale: 5 mv = 0.0034 inch

Series # 4

Lubricant: 2190TEP
Drop Position: 11.75 degrees

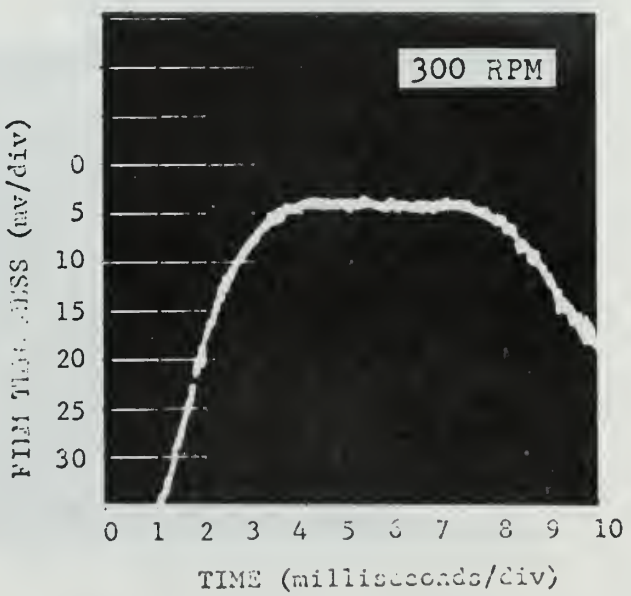

Vertical Scale: 5 mv = 0.0034 inch

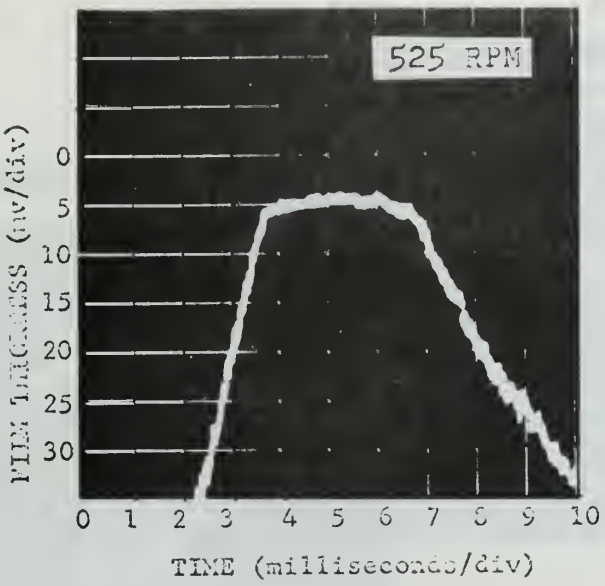

Vertical Scale: 5 mv = 0.0034 inch

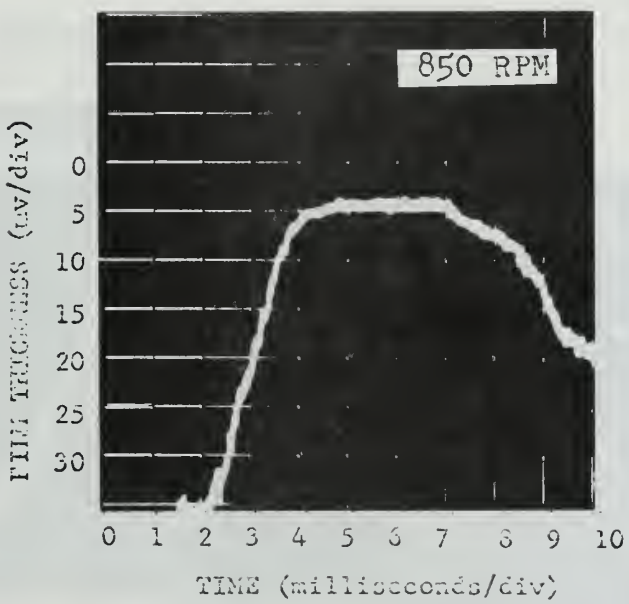

Vertical Scale: 5 mv = 0.0034 inch

Series # 5

Lubricant: Versilube F-50
Drop Position: 7 degrees

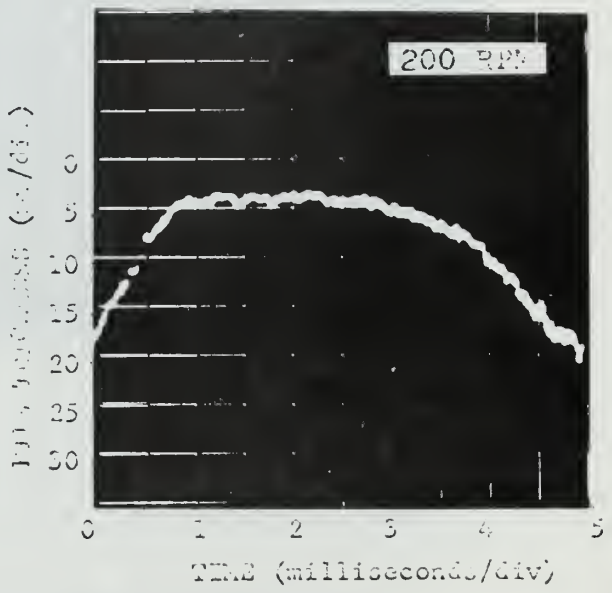

Vertical Scale: 5 mv = 0.00305 inch

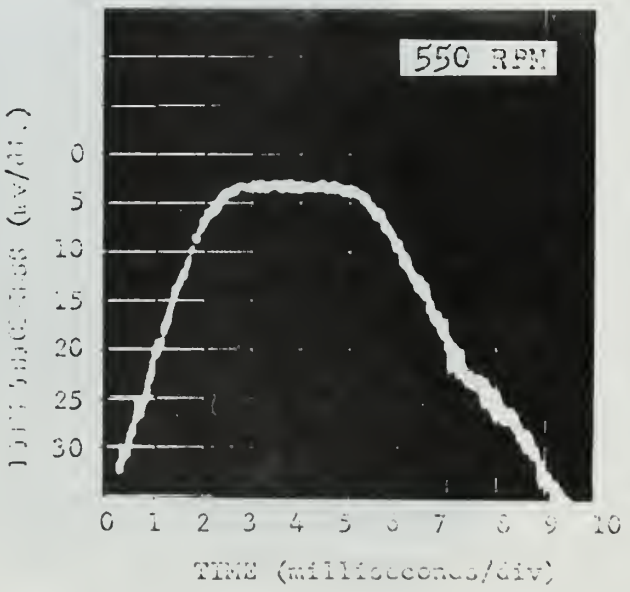

Vertical Scale: 5 mv = 0.00305 inch

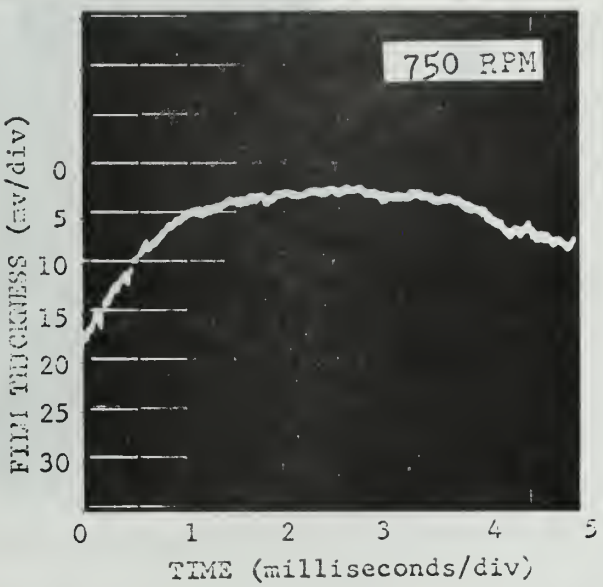

Vertical Scale: 5 mv = 0.00305 inch

Series # 6

Lubricant: Versilube F-50
Drop Position: 11.75 degrees

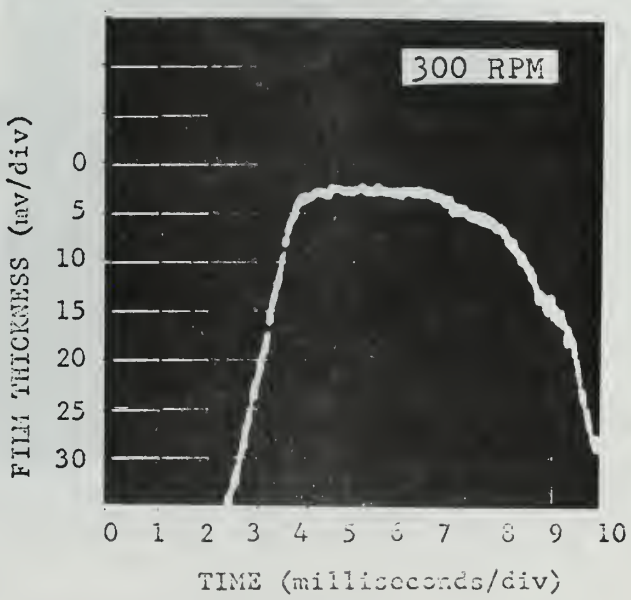

Vertical Scale: 5 mv = 0.00305 inch

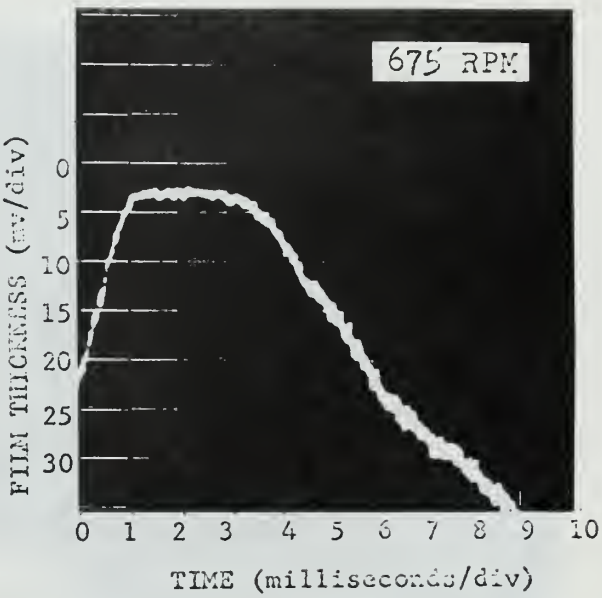

Vertical Scale: 5 mv = 0.00305 inch

Series # 7

Lubricant: 2110TH

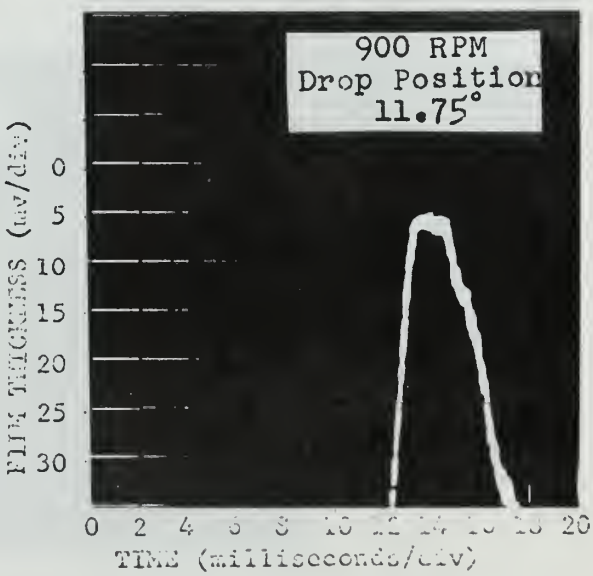

Vertical Scale: 5 mv = 0.0087 inch

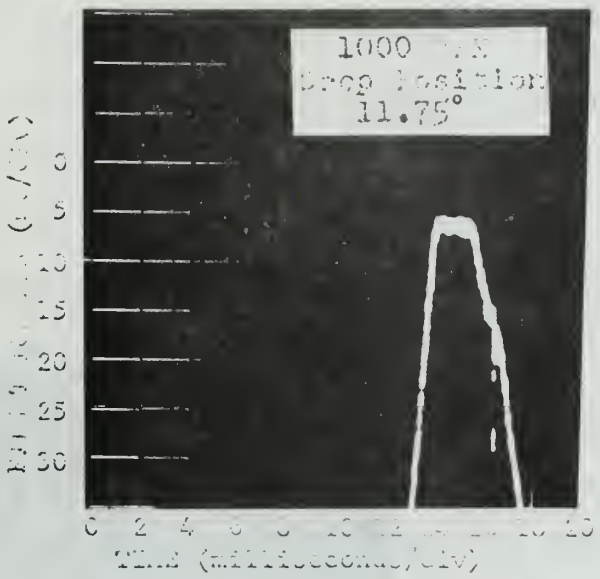

Vertical Scale: 5 mv = 0.0087 inch

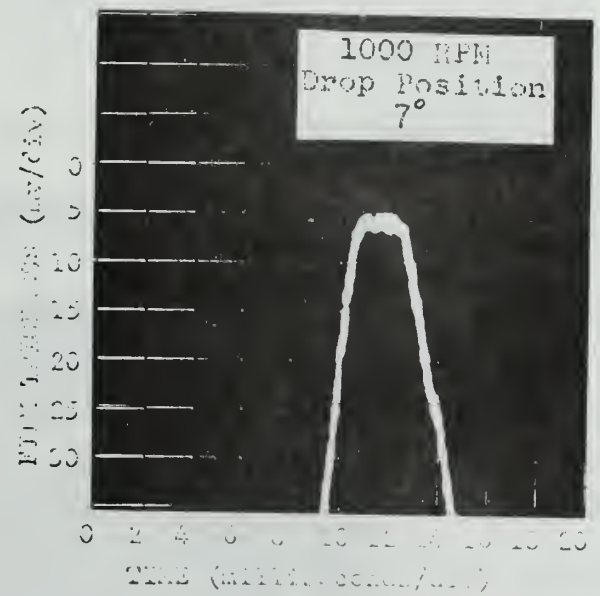

Vertical Scale: 5 mv = 0.0087 inch

Series # 8

Drop Position: 7 degrees

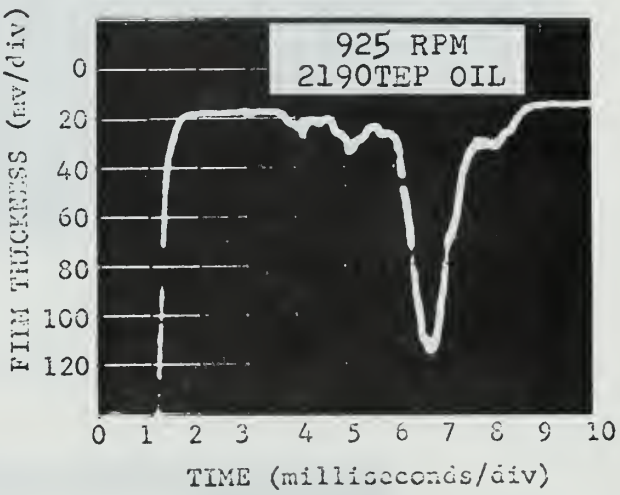

Vertical Scale: 5 mv = 0.0034 inch

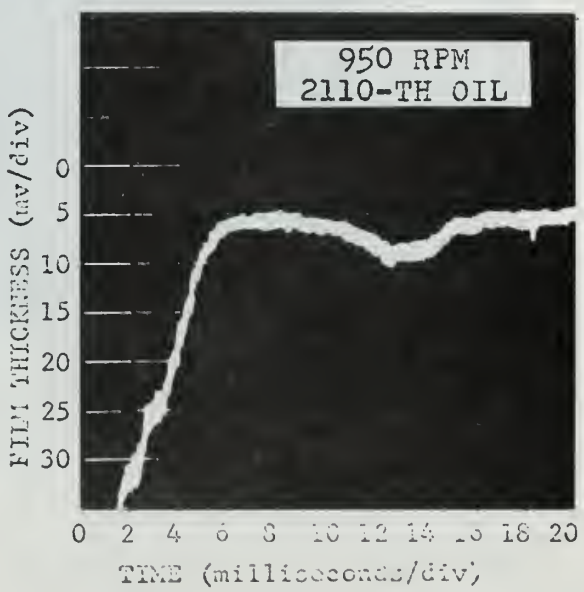

Vertical Scale: 5 mv = 0.0087 inch

8. Discussion of Results.

The results from Series # 1 through # 6 may be utilized for four major purposes:

(1) To obtain minimum film thickness as a function of rotative speed and load.

(2) To obtain the film thickness profile, for given loading conditions, as a function of time.

(3) To obtain the time period during which minimum film thickness is maintained.

(4) To obtain the approach velocity and departure velocity of the pendulum disc.

The first three of these are germane to the problem of film thickness measurement, and will be discussed further. The fourth is applicable to the determination of change in viscosity under load. This application is outlined in Appendix IV.

A plot of film thickness versus rotative speed, with drop height as parameter, is shown in Figures 18, 19 and 20 for the three oils tested. The film thickness is seen, in general, to increase with rotative speed at a constant load. This is in agreement with basic elastohydrodynamic theory [15, 19, 31, 35]. For a given speed, the film thickness is seen to decrease with increase in load for the 2110TH oil and the Versilube F-50 silicone fluid. This conforms to theory. The 2190TEP oil, however, shows the reverse effect with film thickness greater at a greater load up to about 750 rpm. The effect of an extreme pressure additive in the 2190TEP most certainly becomes more prominent at higher loads and would therefore create thicker EP films in that region [10]. However,

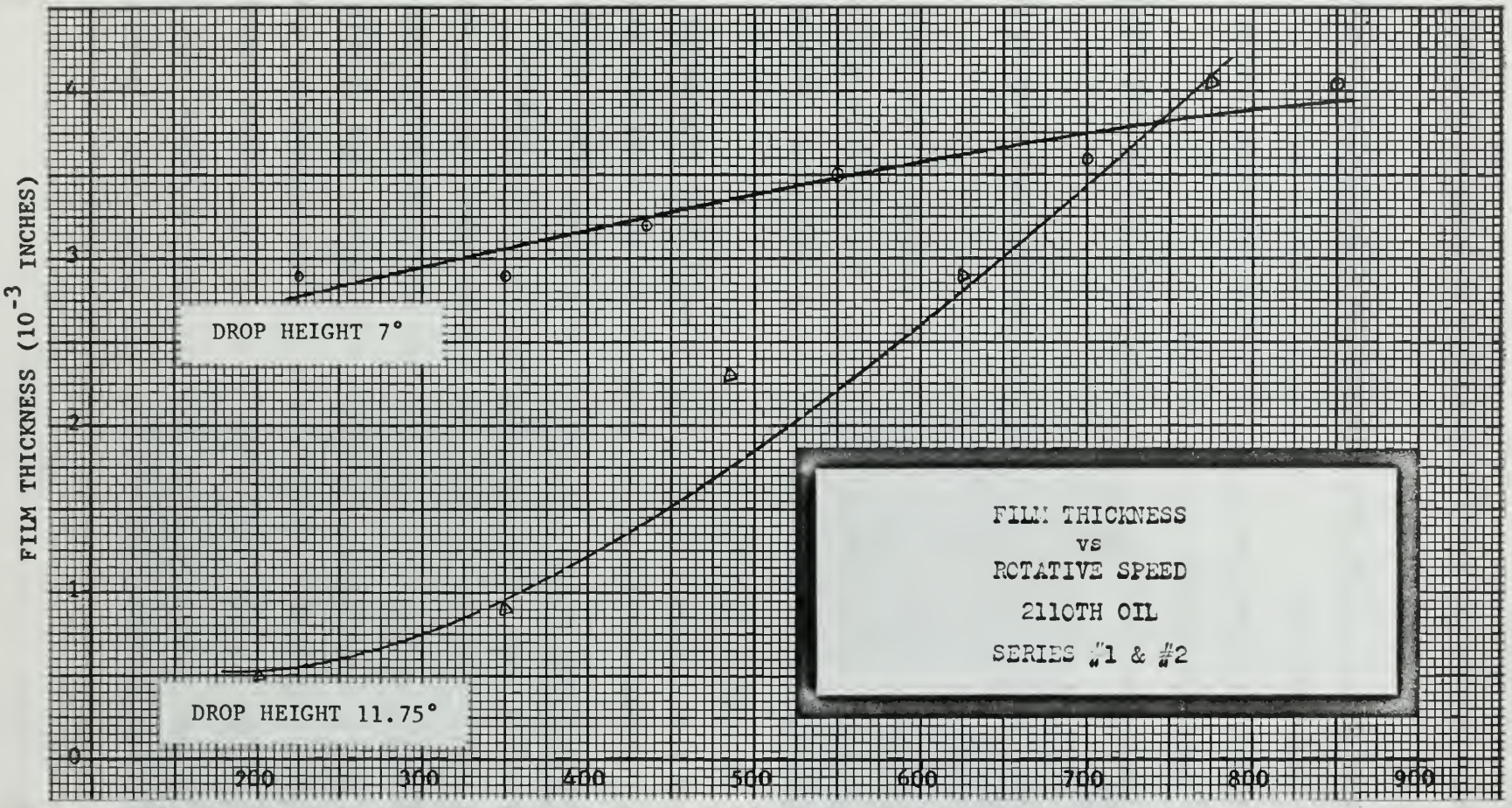
FILM THICKNESS (10^{-3} INCHES)
0
1
2
3
4
200
300
400
500
600
700
800
900
DROP HEIGHT 7°
DROP HEIGHT 11.75°
FILM THICKNESS
vs
ROTATIVE SPEED
2110TH OIL
SERIES #1 & #2
ROTATIVE SPEED (RPM)

FIGURE 18.

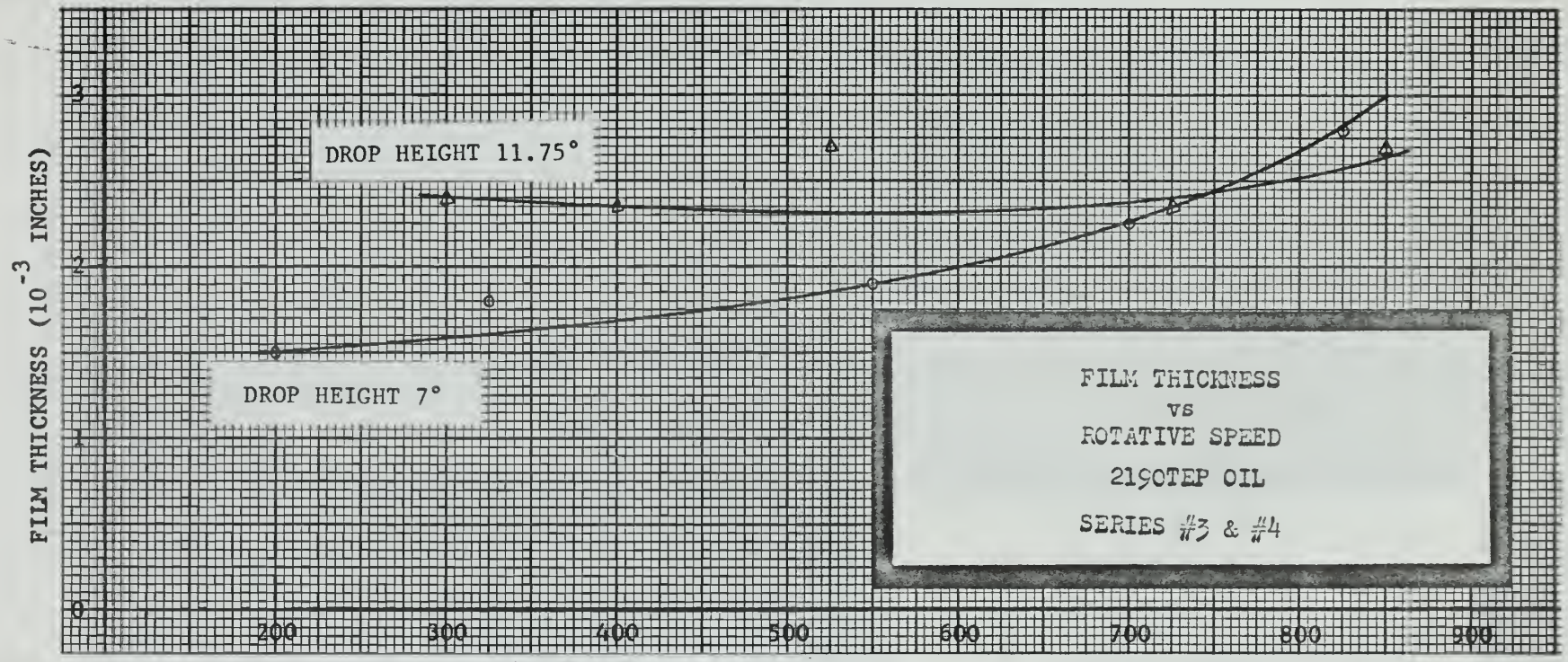
DROP HEIGHT 11.75°
DROP HEIGHT 7°
FILM THICKNESS
vs
ROTATIVE SPEED
2190TEP OIL
SERIES #3 & #4
FILM THICKNESS (10^{-3} INCHES)
3
2
1
0
200
300
400
500
600
700
800
900
ROTATIVE SPEED (RPM)

FIGURE 19.

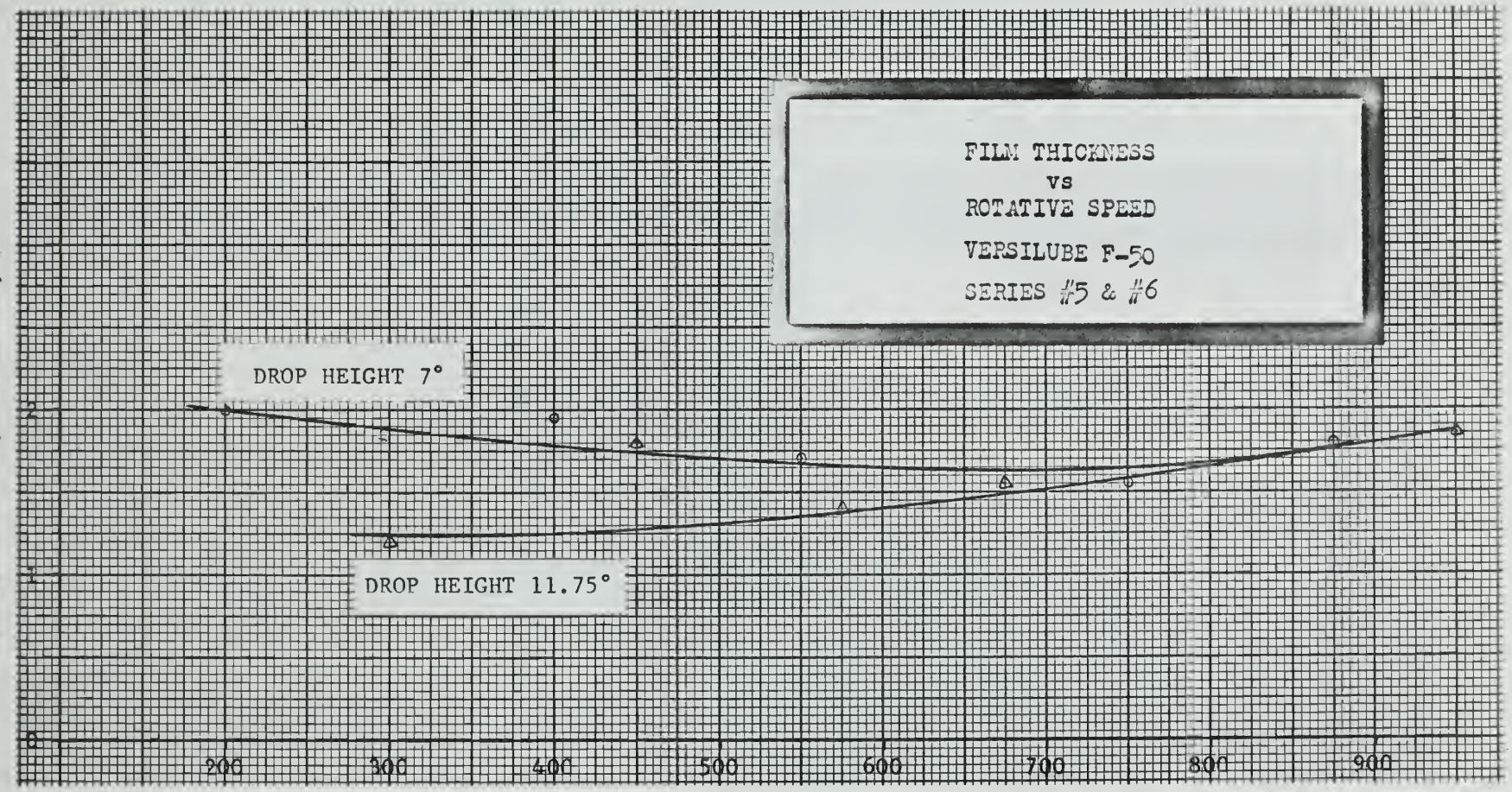

ROTATIVE SPEED (RPM)
FIGURE 20.

it is considered improbable that an EP film alone could account for this reversal.

The film thickness profile as a function of time is a necessary measurement for the determination of both the time period during which minimum film thickness is maintained and the approach velocity and departure velocity of the pendulum disc. Careful inspection of the traces presented indicates that two features are common to all traces:

(1) There exists a time period, of varying magnitude, during which a constant minimum film thickness is maintained.

(2) The slope of the leading edge of the trace is greater than the slope of the trailing edge. Since the slope represents velocity (dx/dt), this shows graphically that the approach velocity is greater than the departure velocity. The validity of this observation is obvious from energy considerations.

To facilitate further discussion, a new term will be defined. **PLATEAU TIME** is defined as the time period during which minimum film thickness is maintained under impact loading conditions. This value may be taken directly from the scaled photographs of thickness versus time. To obtain a comparison of plateau time for the oils tested, a plot of plateau time versus rotative speed, with lubricant type as parameter, was constructed for each load. These curves are shown in Figures 21 and 22. From these curves, it is apparent that plateau time is a function of rotative speed, loading and lubricating fluid. Furthermore, from an intuitive point of view, plateau time would appear to be related to the ability of a lubricant to adhere to the surface of a metal. With these

PLATEAU TIME
vs
ROTATIVE SPEED
DROP POSITION : 7°

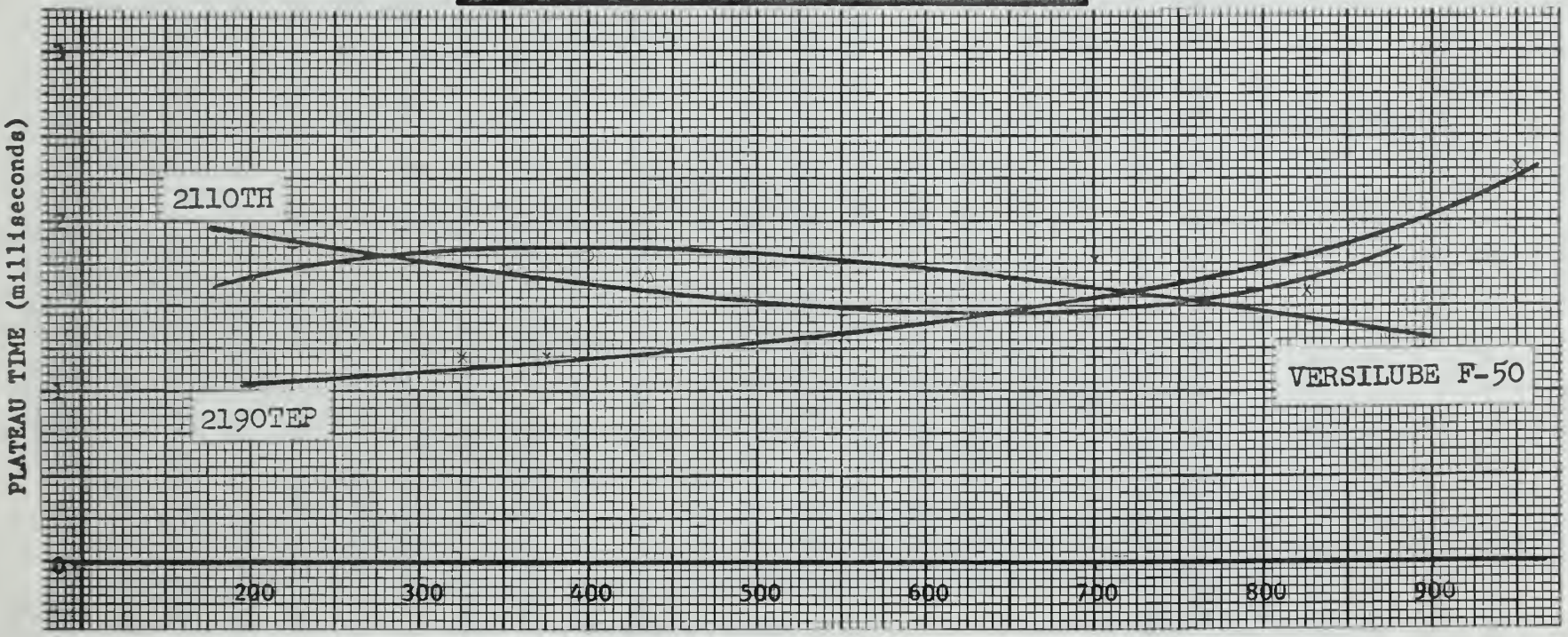

FIGURE 21.

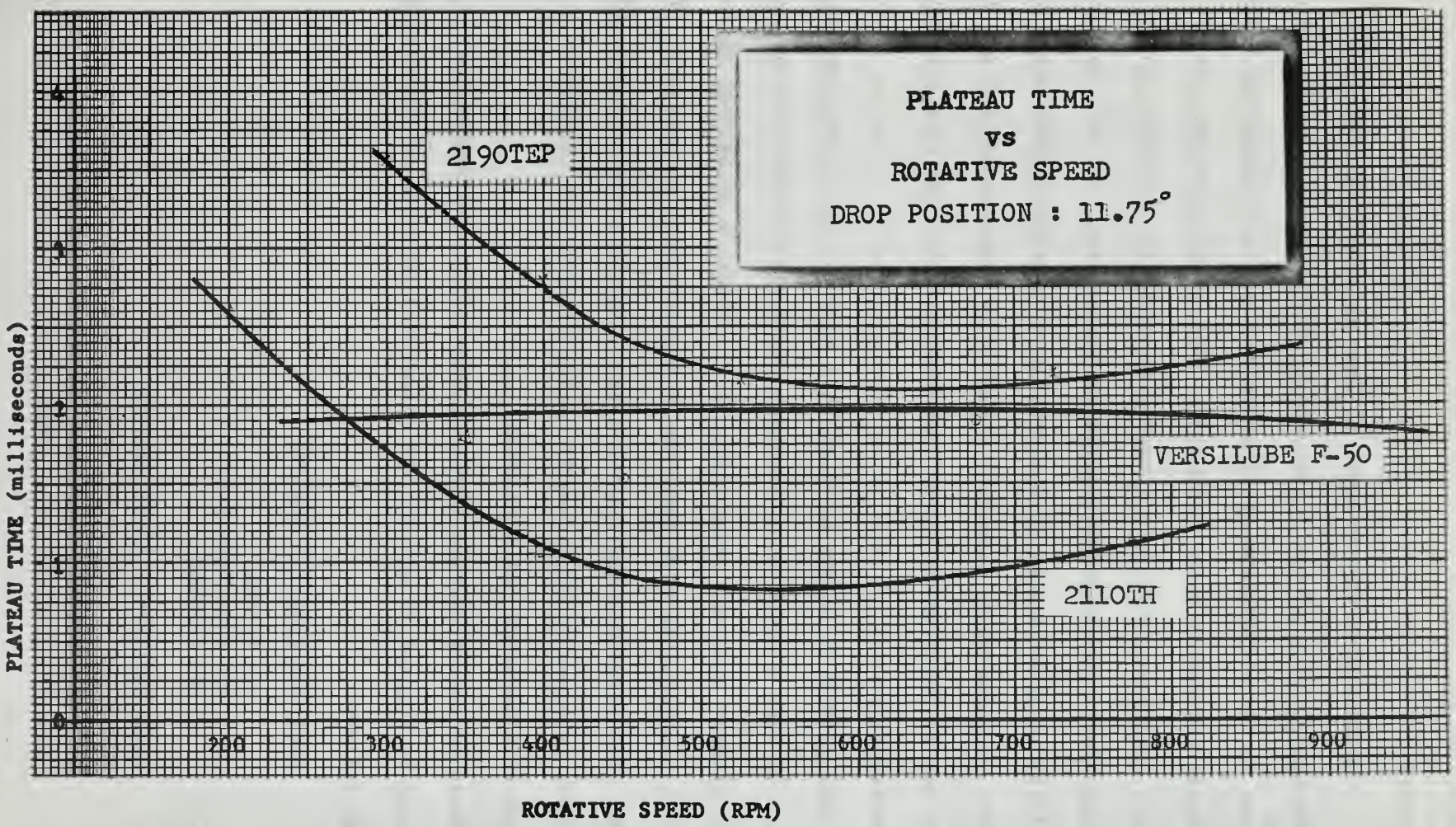
PLATEAU TIME
vs
ROTATIVE SPEED
DROP POSITION : 11.75°
2190TEP
VERSILUBE F-50
2110TH
PLATEAU TIME (milliseconds)
4
3
2
1
0
200
300
400
500
600
700
800
900
ROTATIVE SPEED (RPM)

FIGURE 22.

considerations as a basis, the following interpretation of plateau time is proposed:

Plateau time is a measure of the "oiliness" of a lubricant.

The term "oiliness" was first used by Kingsbury to describe the reduction in the coefficient of friction of a metal surface when wetted with an oil containing polar molecules. When these molecules are present in a lubricant, they form a bond with surfaces, extending their long dimensions roughly perpendicular to the surface. In this manner, several layers of molecules form a coating with reduced coefficient of friction, as compared to a surface wetted with nonpolar molecules. Subsequent use of the term "oiliness" has lead more or less to a synonymity with wettability.

Since plateau time was found to be a function of loading conditions, oiliness is also a function of loading. Test results show no correlation of plateau time with viscosity. Also, there is no pattern of increase in plateau time with increase in viscosity due to pressure. These findings will therefore apply to oiliness. The fact that oiliness is apparently independent of viscosity is in agreement with Kingsbury's original definition of oiliness [23].

Based on the definition herein proposed, the oils tested, as evidenced by Figures 21 and 22, are classified in order of increasing oiliness as follows:

Drop Position - 7 degrees

(1) 2110TH
(2) Versilube F-50
(3) 2190TEP

Drop Position - 11.75 degrees

(1) Versilube F-50

(2) 2110TH
(3) 2190TEP

No attempt will be made in this paper to explain the change in relative oiliness of the oils tested. It is believed that further investigation will be necessary to evaluate this phenomenon.

The results from Series # 7 represent a special group of tests run to show the effect of higher speeds on film thickness. Figures 18, 19 and 20 show a definite trend towards equalization of film thickness, regardless of load, as the rotative speed increases. Figure 20 is perhaps the clearest indication of this. The photographs presented in this series validate the fact that at higher speeds, the speed factor is the dominant variable in the determination of film thickness. This result is in agreement with the findings of Dowson and Higginson [19], which have also been confirmed by Christensen [6].

The photographs in Series # 8 show elastic rebounds from the film. The speed of rotation is a significant factor in causing this effect. It may be noted that elastic rebound did not occur at the lower test speeds. As speed increases, however, the deformation rate of the oil increases during the contact time and the oil responds as an elastic solid. This result was obtained earlier by Borsoff [40].

9. Conclusions.

The thickness of lubricant films under impact loading conditions has been measured as a function of time by passing a collimated beam of light through the film, detecting the emerging light rays, and displaying the transient waveform on a cathode ray oscilloscope. Interpretation of the test results has lead to the following conclusions:

(1) The light measurement technique employed provides a satisfactory method for determination of film thickness.

(2) Results still confirm the fact that rotative speed is the dominant variable in the determination of film thickness in the contact area of rolling cylinders. The effect of load is of a lesser magnitude.

(3) There exists a time period, the magnitude of which is dependent upon rotative speed, load and lubricant type, during which a constant minimum film thickness is maintained at the contact area. This time period has been defined as Plateau Time.

(4) Plateau Time has been interpreted as a measure of the "oiliness" of a lubricant and found to be independent of viscosity.

(5) Further investigation will be necessary to explain fully the mechanism of oiliness.

10. Acknowledgments.

I wish to express my appreciation to Professor E. K. Gatcombe for his professional counsel and guidance in this investigation. Particular thanks are due Professor S. H. Kalmbach for the loan of equipment and advice on design of the optical system and detection system utilized. A commendation goes to Mr. Michael O'Dea of the Machine Facility of the Naval Postgraduate School for his master craftsmanship in the construction of the testing machine.

11. Bibliography.

1. Hersey, M. D. and Shore, H., Viscosity of Lubricants Under Pressure, Mechanical Engineering, Vol. 50, No. 3, March 1928.

2. Hyzer, W. G., Engineering and Scientific High Speed Photography, Macmillan Co., New York, 1962.

3. Janes, R. B. and Glover, A. M., Recent Developments in Phototubes, RCA Review, Vol. 6, No. 1, July 1941, p. 43.

4. Engstrom, R. W., Multiplier Phototube Characteristics; Application to Low Light Levels, Journal of the Optical Society of America, Vol. 37, June 1947, p. 420.

5. Palmgren, A., Ball and Roller Bearing Engineering, published by SKF Industries, Philadelphia.

6. Christensen, H., The Variation of Film Thickness in Highly Loaded Contacts, ASLE Trans. 7, 1964, p. 219.

7. Adkins, R. W. and Radzimovsky, E. I., Lubrication Phenomena in Spur Gears : Capacity, Film Thickness Variation, and Efficiency, ASME Journal of Basic Engineering, Vol. 87, No. 3, p. 655.

8. Tsukizoe, T. and Hisakado, T., On the Mechanism of Contact Between Metal Surfaces - The Penetrating Depth and the Average Clearance, ASME Journal of Basic Engineering, Vol. 87, No. 3, p. 666.

9. Cheng, H. S. and Sternlicht, B., A Numerical Solution for the Pressure, Temperature, and Film Thickness Between Two Infinitely Long, Lubricated Rolling and Sliding Cylinders, Under Heavy Loads, Journal of Basic Engineering, Vol. 87, No. 3, p. 695.

10. Borsoff, V. N. and Wagner, C. D., Studies of Formation and Behavior of an Extreme-Pressure Film, Lubrication Engineering, Vol. 13, No. 2, p. 91.

11. Smith, F. W., Lubricant Behaviour in Concentrated Contact Systems - The Castor Oil-Steel System, Wear, May 1959, p. 250.

12. Hersey, M. D. and Lowdenslager, D. B., Film Thickness Between Gear Teeth - A Graphical Solution of Karlson's Problem, ASME Trans., Vol. 72, 1950, p. 1035.

13. Smith, F. W., Lubricant Behaviour in Concentrated Contact - Some Rheological Problems, ASLE Trans., Vol. 3, No. 1, p. 18.

14. Sibley, L. B. and Orcutt, F. K., Elasto-Hydrodynamic Lubrication of Rolling Contact Surfaces, ASLE Trans., Vol. 4, 1961, p. 234.

15. Grubin, A. N., Fundamentals of the Hydrodynamic Theory of Lubrication of Heavily Loaded Cylindrical Surfaces, Book No. 30, Central Scientific Research Institute for Technology and Mechanical Engineering, Moscow, 1949.

16. Boyd, J. and Robertson, B. P., The Friction Properties of Various Lubricants at High Pressures, ASME Trans., Vol. 67, 1945, p. 51.

17. Deriagin, B. V., Karasev, V. V., Zakhavaeva, N. N., and Lazarev, V. P., Mechanism of Boundary Lubrication and the Properties of the Boundary Lubrication Film, Soviet Physics, Vol. 2, No. 5, p. 980.

18. Gatcombe, E. K., Lubrication Characteristics of Involute Spur Gears - A Theoretical Investigation, Trans. ASME, Vol. 67, 1945, p. 177.

19. Dowson, D., Higginson, G. R., and Whitaker, A. V., Elasto-Hydrodynamic Lubrication : A Survey of Isothermal Solutions, Journal of Mech. Eng. Science, Vol. 4, No. 2, June 1962, p. 121.

20. El-Sisi, S. I., and Shawki, G. S. A., Measurement of Oil-Film Thickness Between Disks by Electrical Conductivity, Jour. of Basic Eng., Vol. 82, No. 1, March 1960, p. 12.

21. El-Sisi, S. I., and Shawki, G. S. A., Performance Characteristics of Lubricating Oil Film Between Rotating Disks, Jour. of Basic Eng., Vol. 82, No. 1, March 1960, p. 19.

22. MacConochie, I. O. and Cameron, A., The Measurement of Oil-Film Thickness in Gear Teeth, Jour. of Basic Eng., Vol. 82, No. 1, March 1960, p. 29.

23. Faires, V. M., Design of Machine Elements, 4th edition, Macmillan Co., New York, 1965.

24. Hall, A. S., Holowenko, A. R., and Laughlin, H. G., Theory and Problems of Machine Design, Schaum Publishing Co., New York, 1961.

25. Eirich, F. R., Rheology - Theory and Applications, Vol. 3, Academic Press, New York, 1960.

26. Kingslake, R., ed., Applied Optics and Optical Engineering, Vol. 1, Academic Press, New York, 1965.

27. Lane, T. B., and Hughes, J. R., A Study of the Oil Film Formation in Gears by Electrical Resistance Measurements, British Journal of Applied Physics, Vol. 3, 1952, p. 315.

28. Siripongse, C., Rogers, P. R., and Cameron, A., Thin Film Lubrication, Engineering, Vol. 186 Part 2, Aug. 1958, p. 146.

29. MacConochie, I. O. and Shakib, I. D., Some Optimum Conditions for the Lubrication of Gear Teeth, ASLE Trans., Vol. 6, 1963, p. 141.

30. Orcutt, F. K., Experimental Study of Elastohydrodynamic Lubrication, ASLE Trans., Vol. 8, No. 4, 1965, p. 381.

31. Cheng, H. S., A Refined Solution to the Thermal-Elastohydrodynamic Lubrication of Rolling and Sliding Cylinders, ASLE Trans., Vol. 8, No. 4, 1965, p. 397.

32. Tallian, T. E., Brady, E. F., McCool, J. I., and Sibley, L. B., Lubricant Film Thickness and Wear in Rolling Point Contact, ASLE Trans., Vol. 8, No. 4, 1965, p. 411.

33. Bornong, B. J., The Effect of Surface Roughness on Fluid Drainage from Metal Surfaces, ASLE Trans., Vol. 7, No. 4, 1964, p. 383.

34. Hersey, M. D., and Hopkins, R. F., Viscosity of Lubricants Under High Pressure - Co-ordinating the Data From Ten Investigations, Mechanical Engineering, Vol. 67, 1945, p. 820.

35. Pinkus, O. and Sternlicht, B., Theory of Hydrodynamic Lubrication, McGraw Hill, New York, 1961.

36. Bridgman, P. W., The Physics of High Pressure, G. Bell and Sons, Ltd., London, 1949.

37. Collins, J. R., The Effect of High Pressure on the Near Infrared Absorption Spectrum of Certain Liquids, The Physical Review, Vol. 36, 1930, p. 305.

38. Veiler, S. Ia. and Likhtman, V. I., Laws Governing Lubrication When Metals Are Worked Under Pressure, Soviet Physics, Vol. 2, No. 5, May 1957, p. 989.

39. Milne, A. A., On the Effect of Lubricant Inertia in the Theory of Hydrodynamic Lubrication, Jour. of Basic Eng., Vol. 81, 1959, p. 239.

40. Borsoff, V. N., On the Mechanism of Gear Lubrication, Jour. of Basic Eng., Vol. 81, 1959, p. 79.

41. Klorig, W. N., An Investigation of Lubricant Film Thickness Under Conditions of High Intensity-Short Duration Loading, USNPGS Thesis, 1965.

42. ASME Pressure-Viscosity Report, Vols. I & II, New York, 1953.

43. Meals, R. N. and Lewis, F. M., Silicones, Reinhold Publishing Corporation, New York, 1959.

44. Klorig, W. N. and Gatcombe, E. K., The Behavior of Suddenly Squeezed Oil Films, Wear, Vol. 9, 1966, p. 93-102.

45. Milne, W. E., Numerical Calculus, Princeton University Press, Princeton, N. J., 1949.

APPENDIX I

LUBRICANT SPECIFICATIONS

1. Military Symbol 2190TEP Petroleum Oil

Mineral Acidity	Neutral
Water	None
Flash Point, degrees F. minimum	350
Pour Point, degrees F. maximum	20
Viscosity	
Centistokes at 100 degrees F.	82-100
Centistokes at 210 degrees F. minimum	8.2

2. Military Symbol 2110TH Petroleum Oil

Mineral Acidity	Neutral
Water	None
Flash Point, degrees F. minimum	325
Pour Point, degrees F. maximum	-10
Viscosity	
Centistokes at 0 degrees F.	2400
Cenistokes at 210 degrees F. minimum	5.3-6.7

3. Versilube F-50 Silicone Fluid

Flash Point, degrees F. minimum	570
Pour Point, degrees F. maximum	-100
Viscosity, centistokes at 210 degrees F.	16
Viscosity-Temperature Coefficient	0.60
Surface Tension, dynes/cm	23

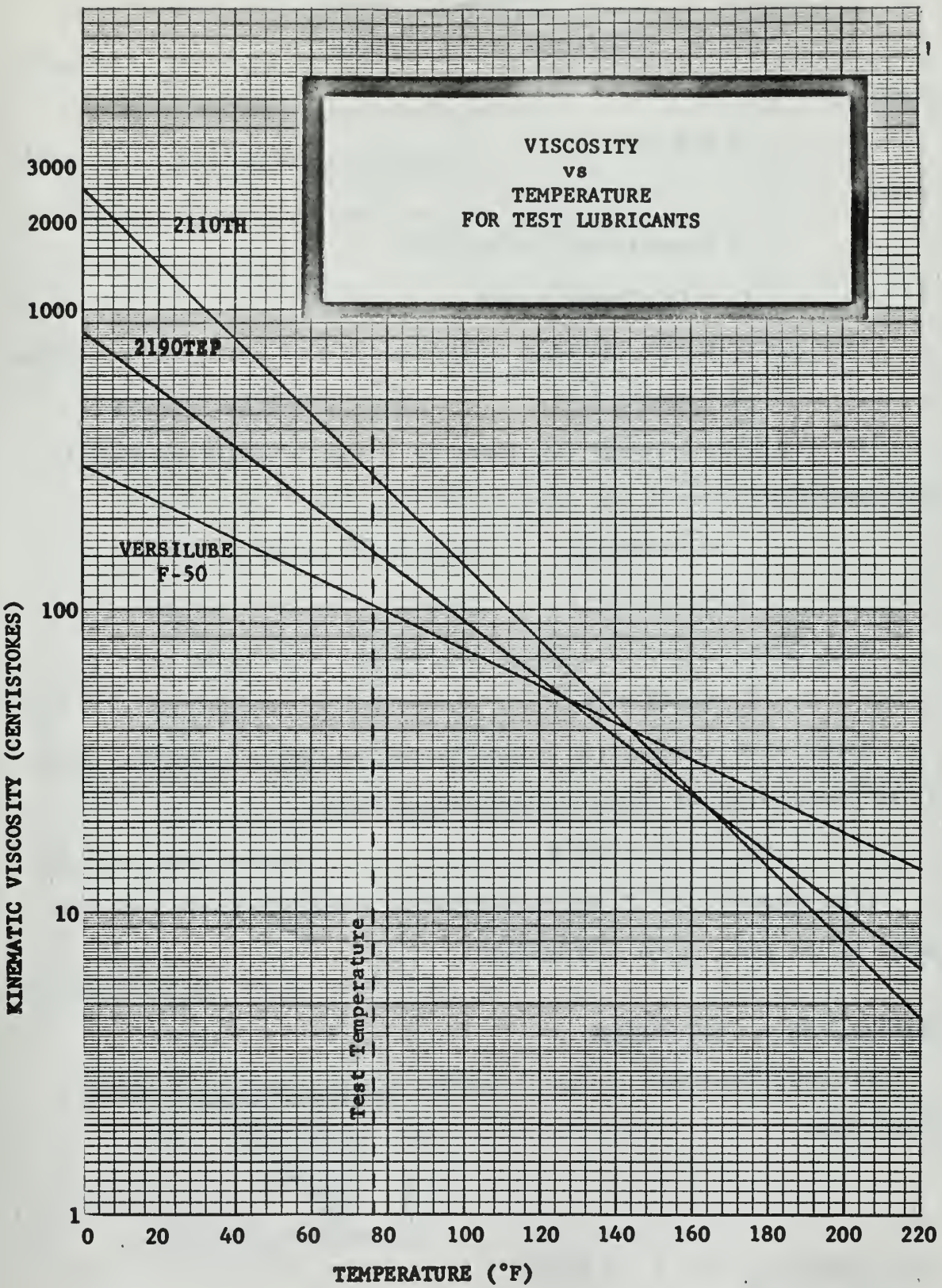
VISCOSITY
vs
TEMPERATURE
FOR TEST LUBRICANTS
2110TH
2190TEP
VERSILUBE
F-50
Test Temperature
KINEMATIC VISCOSITY (CENTISTOKES)
3000
2000
1000
100
10
1
0
20
40
60
80
100
120
140
160
180
200
220
TEMPERATURE (°F)

FIGURE A-1

APPENDIX II

FRICTIONAL DRAG ESTIMATES

Bearings

$$f = T_f/rP \quad \ldots \quad (1)$$

where

f = coefficient of friction

T_f = frictional torque

r = bore radius

P = radial load

For the given bearings (New Departure # 7037 - Single Row Radial Ball Bearing):

$r = 0.2756$ inch

$f = 0.0015$ [5]

Then, from (1):

$$T_f = 4.13 \times 10^{-4} P \quad \ldots \quad (2)$$

Noting that equation (2) applies to one bearing only, we may modify it to account for the two mounting bearings in use:

$$T_f = 8.26 \times 10^{-4} P \quad \ldots \quad (3)$$

From equation (3), T_f may be plotted as a function of P. This is shown by the lower curve in Figure B-1.

Viscous Drag at Test Surface

For one-dimensional fluid flow:

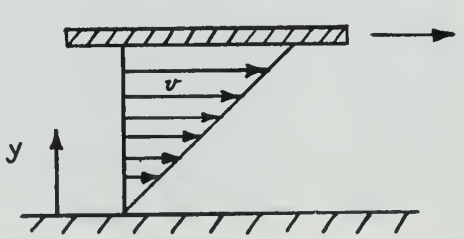

$$\tau = \mu \frac{dv}{dy} \quad \ldots \ldots \ldots \ldots \ldots \ldots \quad (4)$$

where

τ = shear stress in the fluid

μ = absolute viscosity

Equation (4) may be rewritten as:

$$F' = \mu A \frac{\Delta v}{\Delta y} \quad \ldots \ldots \ldots \ldots \ldots \ldots \quad (5)$$

where A is the fluid area being sheared and F' is the shearing force.

Assume the following values:

$\Delta y = 0.0001$ inch

$\mu = 12 \times 10^{-6}$ reyn (SAE 20W at 80°F. and atmospheric pressure)

Speed of driver = 500 RPM

Radius of driver = 3 inches

Radius of driven member = 2 inches

Poisson's ratio = 0.3

Young's modulus = 30×10^{6} psi

$\Delta v = \Delta v_{max}$ = Peripheral speed of driver

From known values:

$$\Delta v = 500\left(\frac{\pi}{30}\right) 3 = 50\pi \text{ (inches/sec)}$$

and equation (5) may be reduced to

$$F' = (50\pi \times 10^{4})\mu A \quad \ldots \ldots \ldots \ldots \ldots \quad (6)$$

We may determine A in the following manner:

Set A equal to the Hertzian contact area

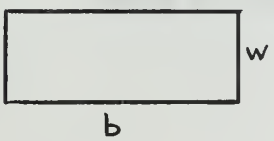

$$A = w \times b \quad \ldots \ldots \quad (7)$$

where b = ½ inch (face width of) (test surface)

and

$$w = \frac{2\, S_{c\ max}}{1/r_1 + 1/r_2} \left(\frac{(1 - \nu_1^2)}{E_1} + \frac{1 - \nu_2^2)}{E_2} \right) \quad \ldots\ldots\ldots\ldots \quad (8)$$

where

$S_{c\ max}$ = maximum Hertzian stress

ν = Poisson's ratio

E = Young's modulus

r_1, r_2 = radii of cylinders in contact

For cylinders of the same material, $\nu_1 = \nu_2$ and $E_1 = E_2$. Equation (8) then reduces to:

$$w = 1.459 \times 10^{-7}\ S_{c\ max} \quad \ldots\ldots\ldots\ldots\ldots \quad (9)$$

The basic formulation for maximum Hertzian stress, assuming a value of 0.3 for Poisson's ratio is

$$S_{c\ max} = \left[\frac{0.35\ F\ (1/r_1 + 1/r_2)}{b(1/E_1 + 1/E_2)} \right]^{\frac{1}{2}} \quad \ldots\ldots\ldots\ldots \quad (10)$$

Inserting known values into (10), we obtain

$$S_{c\ max} = 2.96 \times 10^3\ (F)^{\frac{1}{2}} \quad \ldots\ldots\ldots\ldots\ldots\ldots \quad (11)$$

We may utilize equations (11), (9), (7), and (6) to find F' in terms of μ and F. Then

$$T_f = F'\ r \quad \ldots\ldots\ldots\ldots\ldots\ldots\ldots\ldots \quad (12)$$

where

T_f = frictional torque

r = radius of driven wheel (2 inches)

Combining equations (12), (11), (9), (7), and (6), we have:

$$T_f = 677 \mu\ (F)^{\frac{1}{2}} \quad \ldots\ldots\ldots\ldots\ldots\ldots \quad (13)$$

At this point, we must take into account one of the basic rheological properties of oil - the variation of viscosity with pressure. Data compiled by Hersey and Shore [1] may be used for this purpose. The maximum pressure within the oil film may be found by equating it to the maximum Hertzian compressive contact stress as given in equation (11). Thus, assuming a value of F, a change in μ is determined and T_f in equation (13) may be plotted as a function of F. This is shown in Figure B-1.

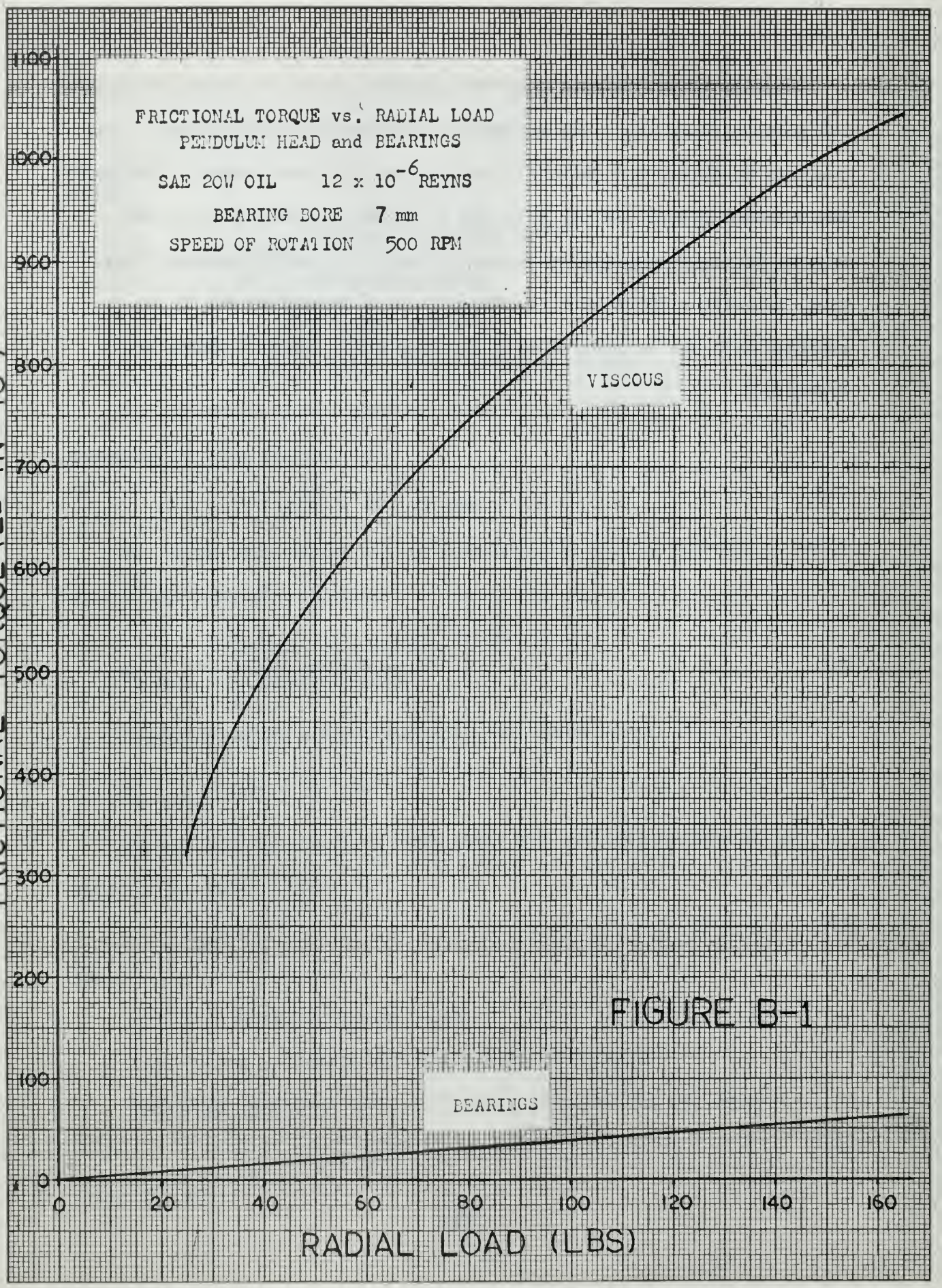
FRICTIONAL TORQUE vs. RADIAL LOAD
PENDULUM HEAD and BEARINGS
SAE 20W OIL 12 x 10^-6 REYNS
BEARING BORE 7 mm
SPEED OF ROTATION 500 RPM
VISCOUS
BEARINGS
FRICTIONAL TORQUE (LB-IN x 10^3)
RADIAL LOAD (LBS)
0
100
200
300
400
500
600
700
800
900
1000
0
20
40
60
80
100
120
140
160

FIGURE B-1

APPENDIX III

CORRELATION OF PENDULUM DROP POSITION AND LOAD

The fundamental principle to be used in correlating drop position and load is that impulse is equal to the change in momentum of a body. The basic quantity to be dealt with is angular momentum, which may be converted to linear momentum. The fact that all motion in this problem is constrained to a single plane permits reduction of the vector equation for angular momentum to the following scalar equation:

$$H_o = I_o \omega \quad . \quad . \quad .

r = 12.00 (inches) ---(from pivot to impact point)

Placing these values in equation (4) yields

$$h_o = 0.0145\ v \quad \ldots\ldots\ldots\ldots\ldots\ldots \quad (5)$$

where the units of v are (inches/second) and h_o is measured in (pound-seconds). The relationship between impulse and momentum may be written as:

$$\Delta h_o = \int_{t_1}^{t_2} F\ dt \quad \ldots\ldots\ldots\ldots\ldots\ldots \quad (6)$$

Making use of equation (5), this may be restated as

$$\int_{t_1}^{t_2} F\ dt = 0.0145\ \Delta v \quad \ldots\ldots\ldots\ldots\ldots\ldots \quad (7)$$

The reason for writing linear momentum in terms of velocity now becomes clear. A value for velocity may be taken from the photographic test results as the slope of the trace (dx/dt) at any point. The problem now remains to evaluate the integral in equation (7). The most direct and appropriate method at hand is the use of numerical differentiation. Equation (7) may be rewritten as:

$$\sum_{o}^{n} F\ \Delta t = 0.0145\ \Delta v \quad \ldots\ldots\ldots\ldots\ldots\ldots \quad (8)$$

Selection of an appropriate number of time intervals, n, and a value of Δt for these intervals permits solution of equation (8) for the radial load, F. If the number of time intervals selected is three, as suggested by Gatcombe [44], use may be made of the following formula from Milne [45]:

$$F = 1/6\ h \left[-2\ y_o + 9\ y_1 - 18\ y_2 \right] \quad \ldots\ldots\ldots \quad (9)$$

where

h = the time interval selected

$$y_o = 0.0145\ v_o$$

$$y_1 = 0.0145\ v_1$$

$$y_2 = 0.0145\ v_2$$

From the foregoing development, it is clear that a single pendulum drop position does not correspond to a unique load on the oil film. Rotative speed has an unmistakable effect on the load being considered inasmuch as it plays a key role in oil residence time in the contact zone.

APPENDIX IV

APPLICATION OF TEST RESULTS TO DETERMINATION OF CHANGE IN VISCOSITY

A change in viscosity may be found by measuring the apparent viscosity of a lubricant under pressure and subtracting from it the viscosity at ambient conditions. The basic approach presented herein will be to measure the torque of the rotating upper disc and equate this to the frictional torque developed in the lubricant film.

The basic equation for the torque of the rotating disc is

$$T = I_o \ddot{\theta} \quad \ldots\ldots\ldots\ldots\ldots\ldots\ldots \quad (1)$$

where

I_o = mass moment of inertia of the disc

$\ddot{\theta}$ = angular acceleration of the disc

Measurement of angular position, θ, with respect to time and subsequent differentiation of this plotted curve will yield a curve of angular acceleration as a function of time. A mean value of angular acceleration over any time period may then be taken as $\bar{\alpha} = 1/t \int_o^t \alpha \, dt$ where the integral simply represents the area under the curve.

From equation (13) of Appendix II

$$T_f = k \mu (F)^{\frac{1}{2}} \quad \ldots\ldots\ldots\ldots\ldots\ldots\ldots \quad (2)$$

where

T_f = frictional torque developed in the oil film

μ = viscosity

F = radial load

k = a constant dependent upon speed of rotation and minimum film thickness.

The value of F may be computed as shown in Appendix III. A value for k may be computed from test results. Then

$$\mu = I_o \ddot{\theta} / k(F)^{\frac{1}{2}} \quad . . . . . \quad (3)$$

It should obviously be noted that the measurement of angular displacement as a function of time is no simple matter. However, a scheme for accomplishing this task might be as follows:

(1) Scribe finely spaced lines on the side edge of the upper disc and blacken the lines.

(2) Focus a light source on the scribed line directly above the point of contact of the two test surfaces.

(3) Image this reflected point, through appropriate optics, on the cathode of a photomultiplier tube.

(4) During contact, the disc will start to rotate, the lines will pass through the focused beam of light, and the photomultiplier will receive a pulsing input with each null corresponding to a line crossing the focus point.

(5) The output of the photomultiplier tube can be coupled, through a resistive load, to an oscilloscope which will display the pulses as a function of time.

(6) Knowing the line spacing and disc geometry will translate the pulse display to angular displacement as a function of time.

INITIAL DISTRIBUTION LIST

		No. Copies
1.	Defense Documentation Center Cameron Station Alexandria, Virginia 22314	20
2.	Library U. S. Naval Postgraduate School Monterey, California	2
3.	Commander, Naval Ship System Command Department of the Navy Washington, D. C. 20360	1
4.	Professor E. K. Gatcombe Department of Mechanical Engineering U. S. Naval Postgraduate School Monterey, California	1
5.	LT Robert M. Hydinger 1341 Rockbridge Avenue Norfolk, Virginia	2
6.	LT Robert L. Towle Box 1474 U. S. Naval Postgraduate School Monterey, California	1
7.	Department of Mechanical Engineering U. S. Naval Postgraduate School Monterey, California	1
8.	Mr. J. R. Belt Head, Friction and Wear Division U. S. Navy Marine Engineering Laboratory Annapolis, Maryland 21402	1

DOCUMENT CONTROL DATA - R&D

(Security classification of title, body of abstract and indexing annotation must be entered when the overall report is classified)

1. ORIGINATING ACTIVITY *(Corporate author)*
U. S. Naval Postgraduate School
Monterey, California

2a. REPORT SECURITY CLASSIFICATION
Unclassified

2b. GROUP

3. REPORT TITLE
The Measurement of Oil Film Thickness Versus Time Under Impact Loading Conditions

4. DESCRIPTIVE NOTES *(Type of report and inclusive dates)*
Thesis

5. AUTHOR(S) *(Last name, first name, initial)*
HYDINGER, Robert M., LT, USN

6. REPORT DATE	7a. TOTAL NO. OF PAGES	7b. NO. OF REFS
May 1966	79	45

8a. CONTRACT OR GRANT NO.	9a. ORIGINATOR'S REPORT NUMBER(S)
N.A.	N.A.
b. PROJECT NO. N.A.	
c.	9b. OTHER REPORT NO(S) *(Any other numbers that may be assigned this report)* N.A.
d.	

10. AVAILABILITY/LIMITATION NOTICES
[redacted]
This document has been approved for public release and sale; its distribution is unlimited.
Mau 4/2/70

11. SUPPLEMENTARY NOTES	12. SPONSORING MILITARY ACTIVITY
N.A.	Commander Naval Ship Systems Command

13. ABSTRACT

The thickness of lubricant films under impact loading conditions has been measured as a function of time by passing a collimated beam of light through the film, detecting the emerging rays with a photomultiplier tube, and displaying the transient waveform on a cathode ray oscilloscope. It is shown that rotative speed is the dominant variable in the determination of film thickness in the contact area of rolling cylinders. Plateau Time is defined as the time period during which minimum film thickness is maintained at the contact area and is interpreted as a measure of the "oiliness" of a lubricant.

DD FORM 1 JAN 64 1473

14. KEY WORDS	LINK A		LINK B		LINK C	
	ROLE	WT	ROLE	WT	ROLE	WT
Oil Film Thickness						

INSTRUCTIONS

1. ORIGINATING ACTIVITY: Enter the name and address of the contractor, subcontractor, grantee, Department of Defense activity or other organization *(corporate author)* issuing the report.

2a. REPORT SECURITY CLASSIFICATION: Enter the overall security classification of the report. Indicate whether "Restricted Data" is included. Marking is to be in accordance with appropriate security regulations.

2b. GROUP: Automatic downgrading is specified in DoD Directive 5200.10 and Armed Forces Industrial Manual. Enter the group number. Also, when applicable, show that optional markings have been used for Group 3 and Group 4 as authorized.

3. REPORT TITLE: Enter the complete report title in all capital letters. Titles in all cases should be unclassified. If a meaningful title cannot be selected without classification, show title classification in all capitals in parenthesis immediately following the title.

4. DESCRIPTIVE NOTES: If appropriate, enter the type of report, e.g., interim, progress, summary, annual, or final. Give the inclusive dates when a specific reporting period is covered.

5. AUTHOR(S): Enter the name(s) of author(s) as shown on or in the report. Enter last name, first name, middle initial. If military, show rank and branch of service. The name of the principal author is an absolute minimum requirement.

6. REPORT DATE: Enter the date of the report as day, month, year; or month, year. If more than one date appears on the report, use date of publication.

7a. TOTAL NUMBER OF PAGES: The total page count should follow normal pagination procedures, i.e., enter the number of pages containing information.

7b. NUMBER OF REFERENCES: Enter the total number of references cited in the report.

8a. CONTRACT OR GRANT NUMBER: If appropriate, enter the applicable number of the contract or grant under which the report was written.

8b, 8c, & 8d. PROJECT NUMBER: Enter the appropriate military department identification, such as project number, subproject number, system numbers, task number, etc.

9a. ORIGINATOR'S REPORT NUMBER(S): Enter the official report number by which the document will be identified and controlled by the originating activity. This number must be unique to this report.

9b. OTHER REPORT NUMBER(S): If the report has been assigned any other report numbers *(either by the originator or by the sponsor)*, also enter this number(s).

10. AVAILABILITY/LIMITATION NOTICES: Enter any limitations on further dissemination of the report, other than those imposed by security classification, using standard statements such as:

(1) "Qualified requesters may obtain copies of this report from DDC."

(2) "Foreign announcement and dissemination of this report by DDC is not authorized."

(3) "U. S. Government agencies may obtain copies of this report directly from DDC. Other qualified DDC users shall request through _____."

(4) "U. S. military agencies may obtain copies of this report directly from DDC. Other qualified users shall request through _____."

(5) "All distribution of this report is controlled. Qualified DDC users shall request through _____."

If the report has been furnished to the Office of Technical Services, Department of Commerce, for sale to the public, indicate this fact and enter the price, if known.

11. SUPPLEMENTARY NOTES: Use for additional explanatory notes.

12. SPONSORING MILITARY ACTIVITY: Enter the name of the departmental project office or laboratory sponsoring *(paying for)* the research and development. Include address.

13. ABSTRACT: Enter an abstract giving a brief and factual summary of the document indicative of the report, even though it may also appear elsewhere in the body of the technical report. If additional space is required, a continuation sheet shall be attached.

It is highly desirable that the abstract of classified reports be unclassified. Each paragraph of the abstract shall end with an indication of the military security classification of the information in the paragraph, represented as *(TS), (S), (C), or (U)*.

There is no limitation on the length of the abstract. However, the suggested length is from 150 to 225 words.

14. KEY WORDS: Key words are technically meaningful terms or short phrases that characterize a report and may be used as index entries for cataloging the report. Key words must be selected so that no security classification is required. Identifiers, such as equipment model designation, trade name, military project code name, geographic location, may be used as key words but will be followed by an indication of technical context. The assignment of links, roles, and weights is optional.

This document has been approved for public
release and sale; its distribution is unlimited.
Mem 4/2/70

[redacted]

thesH975
The measurement of oil film thickness ve
3 2768 002 13316 7
DUDLEY KNOX LIBRARY